Synthesis, *In vitro* Antimicrobial and *In silico* Studies of Aminoalkyl Derivatives of Carvacrol

By: Asaminew Goa (B.Pharm)

Advisors: Dr. Daniel Bisrat (PhD.)

Prof. Kaleab Asres (PhD.)

A Thesis Submitted to the Department of Pharmaceutical Chemistry and Pharmacognosy Presented in Partial fulfillment of the Requirements for the Degree of Master of Sciences in Medicinal Chemistry.

May, 2025

Addis Ababa, Ethiopia

College of Health Sciences

School of Pharmacy

Department of Pharmaceutical Chemistry and Pharmacognosy

Synthesis, *In vitro* Antimicrobial and *In silico* Studies of Aminoalkyl Derivatives of Carvacrol

By: Asaminew Goa (B.Pharm)

A Thesis Submitted to the Department of Pharmaceutical Chemistry and Pharmacognosy Presented in Partial fulfillment of the Requirements for the Degree of Master of Sciences in Medicinal Chemistry.

Advisors: Dr. Daniel Bisrat (PhD.)

Prof. Kaleab Asres (PhD.)

May, 2025

Addis Ababa, Ethiopia

Addis Ababa University

School of Graduate Studies

This is to certify that the thesis prepared by Asaminew Goa, entitled: **Synthesis, *In vitro* Antimicrobial and *In Silico* Studies of Aminoalkyl Derivatives of Carvacrol**" and submitted in partial fulfillment of the requirements for the Degree of Master of Science in Medicinal Chemistry complies with the regulations of the university and meets the accepted standards concerning originality and quality.

Signed by the Examining Committee:

Name	**Signature**	**Date**
External examiner: Dr.Mulugeta Guta (PhD)	----------	----------
Internal examiner: Dr.Wondmagegn Tamiru (PhD)	----------	----------
Advisors: Dr. Daniel Bisrat (PhD)	----------	----------
Prof. Kaleab Asres (PhD)	----------	----------

_____

Chair of the Department

Abstract

Synthesis, *In Vitro* Antimicrobial and *In Silico* Studies of Aminoalkyl Derivatives of Carvacrol

By: Asaminew Goa

Addis Ababa University, 2025

The global rise of antimicrobial resistance has created an urgent need for the development of new antimicrobial agents. Carvacrol, a natural phenolic compound, has drawn significant attention in medicinal chemistry due to its broad-spectrum biological activities. In the present study, two novel aminoalkyl derivatives of carvacrol were successfully synthesized through a Mannich-type reaction, which involves the condensation of carvacrol with formaldehyde and a secondary amine (dimethylamine or piperdine). Structural confirmation of the synthesized derivatives was carried out using spectroscopic techniques (^{1}H-NMR and ^{13}C-NMR). Based on the spectral data, the compounds were identified as 4-((dimethylamino)methyl)-5-isopropyl-2-methylphenol (**14**) and 5-isopropyl-2-methyl-4-(piperidin-1-ylmethyl)phenol (**15**). These compounds were evaluated for their *in vitro* antimicrobial activity against twenty-six bacterial strains and four fungal strains by using disc diffusion and broth dilution methods. Both compound **14** and **15** demonstrated a broad antimicrobial activity. Specifically, Compound **15** exhibited the highest antibacterial activity against *Escherichia coli* and *Vibrio cholerae* strains with a lower MIC value (25 µg/mL) and also showed superior antifungal activity against *Candida albicans* and *Penicillium funiculosum* NCTC 287 (MIC: 200 µg/mL). Furthermore, both compounds were evaluated through *in silico* studies to predict their potential mechanisms of action and assess their drug-likeness properties. Among the two, compound **14** exhibited the strongest binding affinity, with a docking score of -5.677 kJ/mol against the target protein enoyl-

acyl carrier protein reductase (FabI), a crucial enzyme in bacterial fatty acid biosynthesis. This work suggests that the aminoalkyl derivatives of carvacrol could be promising candidates for the development of new antimicrobial drugs that combat infections and help combat antimicrobial resistance.

Keywords: Carvacrol, Aminoalkyl, Antimicrobial, Antimicrobial Resistance (AMR), Antibacterial, Antifungal, *In Silico* study

Acknowledgments

First and foremost, I am profoundly grateful to Almighty GOD for blessing me with good health, strength, and resilience throughout my life's journey.

I would like to express my heartfelt gratitude and deep respect to my advisor, Dr. Daniel Bisrat (PhD), for his invaluable guidance and unwavering support. I am also sincerely thankful to Prof. Avijit Mazumder of the Central Drugs Laboratory and the Institute of Microbial Technology in Kolkata, India, for evaluating the antimicrobial activity of the synthesized compounds. My appreciation also goes to Prof. Kaleab Asres for his support. My appreciation extends to the Department of Pharmaceutical Chemistry and Pharmacognosy, Addis Ababa University, for providing me with the opportunity to carry out this research. I also gratefully acknowledge Wolaita Sodo University for sponsoring my MSc studies.

Finally, I extend my sincere thanks to all my family members for their constant encouragement and support, which played a crucial role in the successful completion of this thesis.

Table of Contents

Contents

List of Figures

List of Schemes

List of Tables

List of Abbreviations

^{1}H NMR	Proton Nuclear Magnetic Resonance
^{13}C NMR	Carbon Thirteen Nuclear Magnetic Resonance
ADMET	Absorption Distribution Metabolism Excretion and Toxicity
AIDS	Acquired Immunodeficiency Syndrome
AMR	Antimicrobial Resistance
ATCC	American Type Culture Collection
ATP	Adenosine Triphosphate
$CDCl_3$	Deuterated Chloroform
CYP450	Cytochrome P450
DNA	Deoxyribonucleic Acid
EAS	Electrophilic Aromatic Substitution
FAS	Fatty Acid Synthase
FDA	Food and Drug Administration
MDR	Multidrug-Resistant
MHz	Megahertz
MIC	Minimum Inhibitory Concentration
NADH	Nicotinamide Adenine Dinucleotide
NCTC	National Collection of Type Cultures
NMR	Nuclear Magnetic Resonance
PDB	Protein Data Base

PH	Power of Hydrogen
PPM	Parts per Million
SDF	Structure-Data Format
SMILES	Simplified Molecular-Input Line-Entry System
TLC	Thin layer Chromatography
USA	United States of America
UV	Ultraviolet
WHO	World Health Organization
ZOI	Zone of Inhibition

1. Introductions

1.1. Infectious Diseases

1.1.1. Overview of infectious Diseases

Infectious diseases, caused by harmful microorganisms such as bacteria, viruses, fungi, and parasites, have been a significant cause of morbidity and mortality throughout human history. These diseases occur when pathogens invade the body, multiply, and disrupt normal biological functions, often resulting in a variety of symptoms ranging from mild to severe (Metrics, 2020; Verhoef et al., 2019). Despite advancements in medicine, infectious diseases remain a significant global health concern, particularly in low-income countries and among vulnerable populations such as young children. According to a 2007 WHO report, infectious diseases are spreading rapidly than ever before and new infectious diseases are being found more frequently than ever before (WHO, 2007).

In 2019, "Global Comprehensive Estimates of the Burden of Bacterial Infections" found that 33 different types of bacteria caused 7.7 million deaths globally. In addition, bacterial infections are the second leading cause of death globally, after ischemic heart disease. The five leading pathogens that caused mortality among the investigated bacteria were *Staphylococcus aureus*, *Escherichia coli*, *Streptococcus pneumoniae*, *Klebsiella pneumoniae*, and *Pseudomonas aeruginosa*. *Staphylococcus aureus* and *Escherichia coli* are two of the most clinically important bacterial pathogens, responsible for a wide range of serious infections and contributing significantly to the global burden of antimicrobial resistance (Ikuta, 2022).

Fungal diseases can have various clinical effects since they can result in life-threatening infections and sight-threatening, as well as substantial morbidity in the case of chronic fungal

diseases (Denning, 2024). Over 1.5 million individuals are killed by fungal diseases globally per year, which also impacts over a billion people. Serious fungal infections may occur from a variety of medical conditions such as cancer, AIDS, asthma, organ transplantation, and corticosteroid treatments. Infections in these patients have the potential to worsen quickly, leading to increased morbidity and mortality (Bongomin et al., 2017).

Certain germs are no longer susceptible to the majority of medications now in use because of inadequate infection treatment, unnecessary antibiotic prescriptions, and improper administration by patients. As a result, treating infections becomes increasingly challenging as the antibiotics and other antimicrobial medications that have been utilized up to this date are no longer effective (Annunziato, 2019).

Natural products have long served as valuable sources of therapeutic leads, with many offering unique mechanisms of action against resistant pathogens. Among these natural compounds, carvacrol, a monoterpenoid phenol found abundantly in the essential oils of oregano and other aromatic plants, exhibits antimicrobial activities (Hao et al., 2021). However, its clinical potential is limited by volatility, low aqueous solubility, and low bioavailability (Baranauskaite et al., 2018). To overcome these limitations and enhance its biological activity, chemical modification of carvacrol through the Mannich-type reaction is considered an important strategy. The Mannich-type reaction is a three-component condensation in which a compound containing an active hydrogen atom reacts with formaldehyde and an amine, with the elimination of a water molecule, resulting in the formation of an aminoalkylated product (Bhardwaj et al., 2018).In this study, aminoalkyl derivatives of carvacrol were synthesized using secondary amines such as dimethylamine and piperidine.

1.1.2. **Antimicrobial Resistance**

Antimicrobial resistance (AMR) is a worldwide concern. WHO lists it as one of the top ten global public health risks that humanity is now facing. Antibiotic resistance occurs when germs develop to adapt to the effects of drugs designed to eradicate them (WHO, 2023). Infections caused by multidrug resistant organisms (MDROs) which result in significantly fewer number of treatment options, making them one of the main global public health concerns (Gnimatin et al., 2022). Although the discovery of antibiotics has transformed to fight against life-threatening diseases, the emergence and spread of antibiotic resistance causes people to die from diseases that cannot be cured all over the world these days. According to a Lancet study, bacterial AMR caused an estimated 1.05 million deaths in 2019 and was directly responsible for 250,000 deaths in the African region. With 23.7 deaths per 100,000, sub-Saharan Africa is the region most affected by AMR, despite it being a global problem. *Escherichia coli* was the leading pathogen causing deaths associated with resistance, followed by *Staphylococcus aureus, Klebsiella pneumoniae*, *Streptococcus pneumoniae*, *Acinetobacter baumannii*, and *Pseudomonas aeruginosa* (Sartorius et al., 2024). Ethiopia also has a high rate of antibiotic resistance, with common pathogens such as *Enterococcus species, S. aureus, E. coli, K. pneumonia,* and *P. aeruginosa* being resistant to key antimicrobial drugs (Berhe et al., 2021).

1.2. **Statement of the problem**

Antimicrobial resistance (AMR) has emerged as one of the most pressing global health threats of the 21st century. The rise of pathogens resistant to nearly all classes of antimicrobial drugs has led to increased morbidity, mortality, and economic burden (Prashanth et al., 2021; Salam et al., 2023). In 2019 alone, an estimated 1.27 million deaths were directly linked to bacterial AMR, with projections suggesting up to 10 million annual deaths by 2050 if current trends continue

(Wah et al., 2023). This crisis is compounded by the limited pipeline of new antibiotics and the growing ineffectiveness of existing treatments. The World Health Organization has emphasized the urgent need for research into new antimicrobial agents to combat this escalating threat. (WHO, 2011).

In addition to bacterial resistance, antifungal treatments face similar challenges, with limited drug classes, increasing resistance, and side effects complicating both prevention and treatment (Frieri et al., 2016). Notably, most antifungal drugs introduced in the past decade belong to existing classes, highlighting the lack of innovation (Memar et al., 2017; Vitiello et al., 2023). These issues underscore the critical need to develop novel, effective, and safer antimicrobial compounds to address both bacterial and fungal infections in an era of rising resistance.

Natural products such as carvacrol have attracted attention due to their broad-spectrum antimicrobial potential. However, their direct application is often hindered by physicochemical limitations, including high volatility, poor aqueous solubility, and low bioavailability. These drawbacks reduce their therapeutic utility, emphasizing the need for structural modification to enhance their bioavailability, stability, and antimicrobial efficacy.

1.3. Literature Review

1.3.1. Chemistry and physico-chemical properties of carvacrol

Carvacrol is chemically known as 2-methyl-5-(1-methylethyl)-phenol, represents a liquid monoterpenoid phenol that is isomeric to thymol (Rad et al., 2018). According to the International Union of Pure and Applied Chemistry, it is also known as 5-isopropyl-2-methylphenol (National Center for Biotechnology Information, 2023). It is chemically related to phenolic compounds, with the molecular formula $C_{10}H_{14}O$ and a molecular weight of 150.22. It

exhibits lipophilic properties with a density of 0.976 g/ml at room temperature and a boiling point of 236–237 °C. Carvacrol is highly soluble in ethanol, acetone, and diethyl ether but insoluble in water (Mohammedi, 2017).

1.3.2. **Antimicrobial activity of carvacrol derivatives**

Carvacrol is a naturally occurring monoterpenoid phenol, primarily found in the essential oils. This organic compound is produced by a variety of aromatic plants such as oregano (*Origanum vulgare*), thyme (*Thymus vulgaris*), *Coridothymus, Thymbra, Satureja,* and *Lippia* (Herrera-calderon et al., 2020). It is known for its distinctive odor, often described as warm, spicy, and medicinal, and its various biological activities, including antimicrobial, antioxidant, anti-inflammatory, and anticancer properties. These beneficial effects have led to increasing interest in carvacrol and its derivatives as potential candidates for the pharmaceutical, food, and cosmetic industries (Bendre et al., 2018; Zaman et al., 2024).

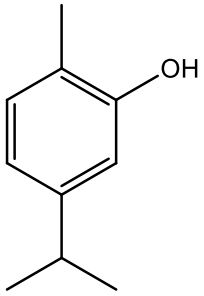

Carvacrol (**1**)

Figure 1: Chemical structure of carvacrol

The FDA has approved carvacrol for use in food, and the Council of Europe has categorized it as a Category B chemical flavoring agent that can be added to food at levels of 2 parts per million in beverages, 5 parts per million in flakes, and 25 parts per million in candies (Vincenzi et al.,

2004). Carvacrol is also utilized as a component in mouthwash, cosmetics, and perfumes. Some of these products are designed to massage joints and treat nail fungus as topical ointments. It has also been formulated into drugs to treat mouth and throat infections and to prevent gingivitis (Memar et al., 2017).

Carvacrol and its derivatives are effective against many strains of bacteria and fungi that are harmful to human health or cause significant financial losses (Wanda, 2023). Several biological activities, such as antifungal, antibacterial, anti-cancer, and antioxidant properties, have been reported. Carvacrol has been studied extensively as an antibacterial agent in food to control both gram-positive and gram-negative bacteria (Sawan et al., 2024; Sisto et al., 2020). It has strong antibacterial activity against all tested oral pathogens, with MICs ranging from 0.625 to 10.0 mg/mL; the highest efficacy was observed against *Candida albicans* and *Streptococcus mutans* (Baser, 2008).

Several carvacrol derivatives were synthesized; among them, ether derivatives **(2)** were synthesized by Nikumbh et al., (2003) using both saturated and unsaturated aliphatic side chains along with aromatic units. These derivatives showed strong antibacterial action against strains of both Gram-positive and Gram-negative bacteria; when compared to carvacrol, the carboxymethyl derivative was the most effective. Similarly, carvacryl ester derivatives **(3)** were synthesized and evaluated for their antifungal activity. The methanoyl and 2-chloromethanoyl groups exhibited the highest anticandidal action against *Candida albicans*, as shown with MICs of 0.25 mg/mL (Lazarević et al., 2022).

Introducing selected amines into the carvacrol aromatic ring, which had been treated with chlorosulfonic acid, these were also new sulfonamides derived from carvacrol. These derivatives

exhibited antimicrobial activity consistently stronger than carvacrol against selected *Staphylococcus aureus* strains and helped reduce bacterial resistance. Derivatives **(4a)**, **(4b)**, and **(4c)**, which contained p-toluene, p-fluorobenzene, and 4-amino-N-(thiazol-2-yl) benzene sulfonamide as substituents, respectively, showed MIC values ranging from 3.90 to 62.50 ppm, the lowest among the tested compounds (Oliveira et al., 2016).

Allyl carvacrol derivatives **(5)** showed a MIC equal to 62.5 µg/ml, except for the ortho allyl carvacrol derivative **(6)**, which exhibited the most significant improvement in activity against *Propionibacterium acnes* (MIC of 31.25 µg/ml). Alkyl carvacrol derivatives **(7)** also demonstrated notable inhibitory effects, with MIC values ranging from ≤ 15.6 to 31.25 µg/ml, although *Staphylococcus aureus* exhibited greater resistance to the ortho propyl carvacrol derivative (MIC value: 125 µg/ml) (Marinelli et al., 2018).

Carvacrol codrug derivatives by direct co-drug strategy **(8-11)**, where the hydroxyl group of carvacrol was conjugated via an ester bond to the carboxyl group of sulfur-containing amino acids. Derivative **(8)** exhibited the most significant enhancement in antibacterial activity, showing MIC values of 2.5 mg/mL for all bacterial strains tested, except *P. aeruginosa*. When tested against *Candida albicans*, carvacrol codrugs **(9)**, **(10)**, and **(11)** demonstrated fungicidal activities with MIC values of 0.15, 0.3, and 0.6 mg/mL, respectively (Cacciatore et al., 2015).

In a study conducted by Alokam et al., (2014), various carvacrol derivatives, including 4-chlorocarvacrol derivatives, were synthesized and evaluated for their potential as inhibitors of *Mycobacterium tuberculosis* chorismate mutase. Specifically, 4-chlorocarvacrol derivatives **(12)** exhibited significant inhibitory effects against *M. tuberculosis* strains (MIC = 67.69 µM) and showed promising antimycobacterial activity. These derivatives showed improved binding

affinity to the enzyme due to the electron-withdrawing properties of the chloro substituent, which facilitated better interactions with the active site of the enzyme.

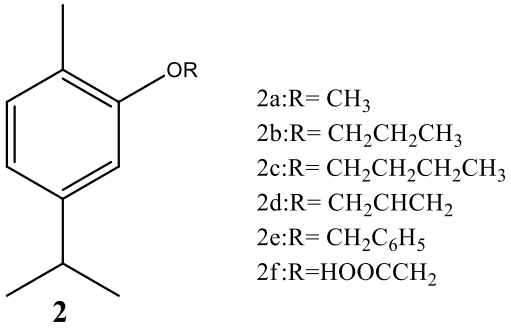

Figure 2: Ether derivatives of carvacrol

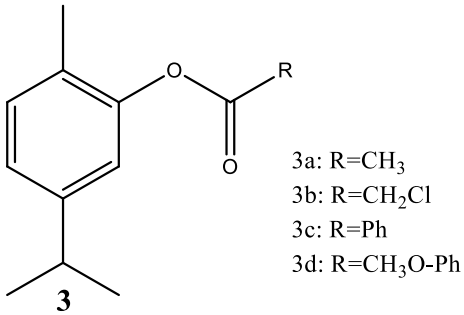

Figure 3: Carvacryl ester derivatives as antifungal agents

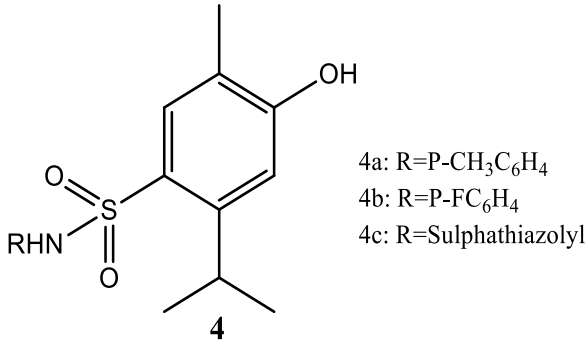

Figure 4: Sulfonamides derived from Carvacrol

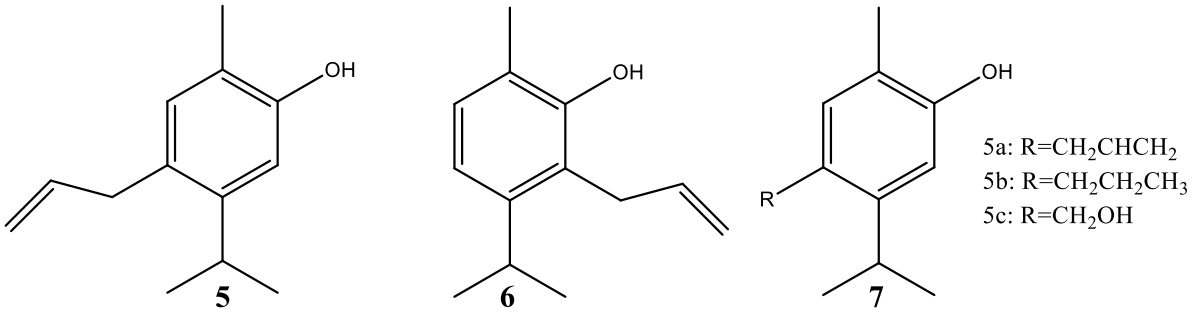

Figure 5: Allyl and alkyl carvacrol derivatives

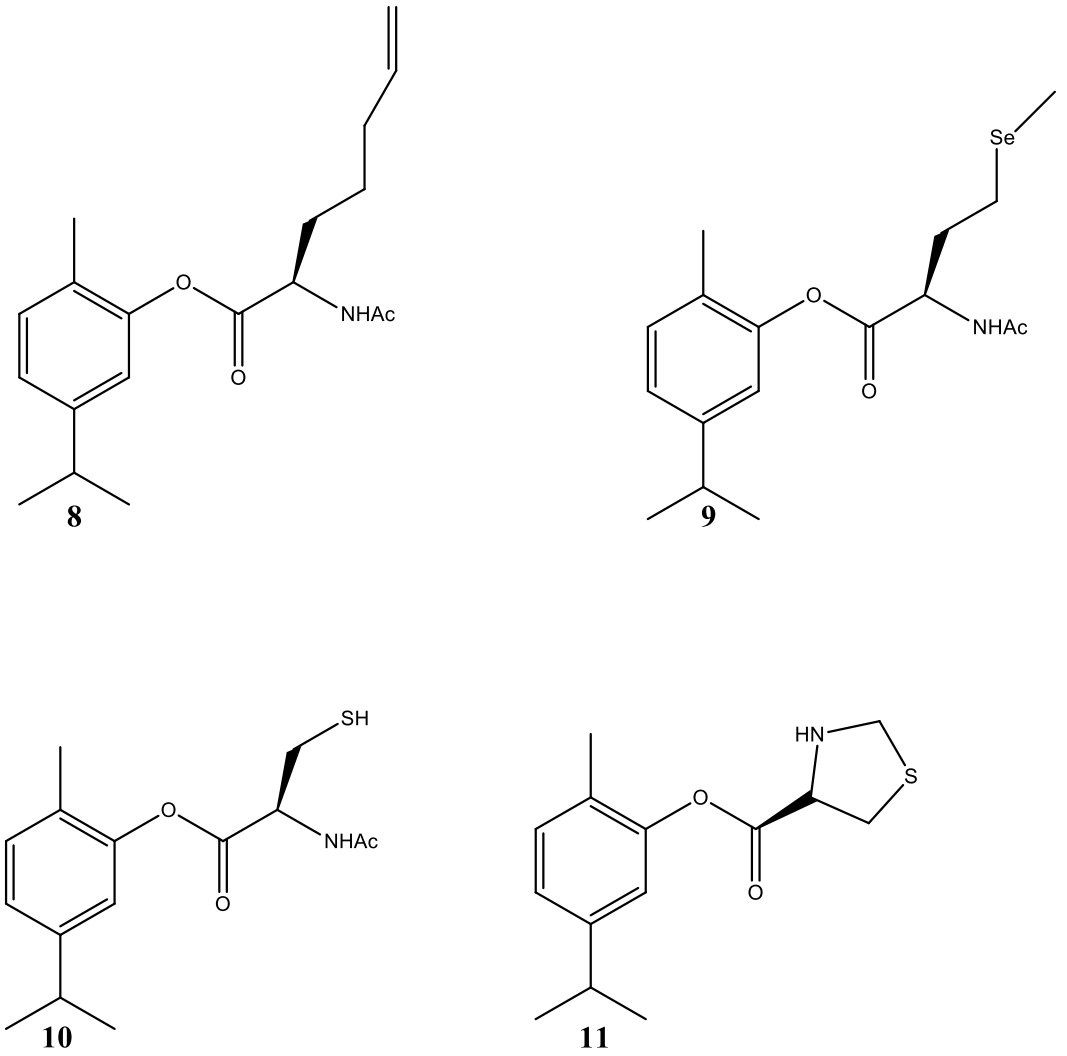

Figure 6: Carvacrol codrug derivatives by direct co-drug strategy

1.3.3. **Antimicrobial mechanism of action of carvacrol derivatives**

*1.3.3.1. **Antibacterial mechanisms***

1.3.3.1.1. **The disruption of the cell membranes**

Carvacrol and its derivatives are able to effectively manage an infection-related disease, which is well established, although the molecular mechanisms behind its antibacterial action are still unclear. One of the key mechanisms by which it exerts antimicrobial activity is by disrupting the cell membranes of bacteria and fungi. The phenolic group of carvacrol is believed to work with the fatty layer of microbial membranes, making them more permeable and causing important substances inside the cells, like ions and small molecules, to leak out. This leads to cell death (Marinelli et al., 2018).

Antibacterial drugs that target and disrupt the bacterial cell membrane represent a vital strategy in the fight against infections, especially those caused by multidrug-resistant bacteria. Polymyxins, daptomycin, and lipopeptides are the primary drugs that act on the bacterial membrane, causing leakage of intracellular contents and cell death. While these drugs are effective against resistant pathogens, they are often limited by toxicity concerns such as nephrotoxicity, neurotoxicity, and muscle toxicity. Ongoing research aims to develop new agents with improved efficacy and safety profiles, as well as to overcome bacterial resistance mechanisms (Fu et al., 2020; Silverman et al., 2003).

1.3.3.1.2. **Depletion of intracellular ATP**

Ultee et al. hypothesized a scheme on the mechanism by which carvacrol enters the bacterial cytoplasmic membrane. According to this theory, undissociated carvacrol dissociates and diffuses through the cytoplasmic membrane before releasing its proton into the cytoplasm. After

returning undissociated with a potassium ion, it exits the membrane and enters the external environment. Carvacrol returns to the cell after substituting a proton for potassium outside of it (Ultee et al.,2002).

The antibacterial activity of carvacrol has also been demonstrated to depend on its current free hydroxyl and delocalized electronic systems. When carvacrol enters the bacterial cytoplasm, the delocalized lone electron pair on its hydroxyl oxygen can form with its benzene ring to produce a p-π conjugate. This enhances the acidity of the bacterial cytoplasm by encouraging the release of a proton on the phenolic hydroxyl group. However, the cytoplasm's pH is typically very close to neutral. To maintain the right pH inside the cell, bacteria must use ATP to move extra protons out of the cell. Cell death results from this, which eventually exhausts the intracellular ATP pool. The decrease of intracellular ATP is therefore one of carvacrol's primary antibacterial actions (Suntres & Coccimiglio, 2013).

1.3.3.1.3. **Enoyl- acylcarrier protein reductase (FabI)**

The biosynthesis of fatty acids is a crucial initial step in the production of membrane lipids and plays an essential role in bacterial physiology. In most bacteria and plants, fatty acid synthesis is carried out by a distinct and highly conserved set of enzymes known as the Type II, or dissociated, fatty acid synthase (FAS) system. This system is structurally and functionally different from the Type I FAS system found in mammals, where all the enzymatic reactions occur within a single multifunctional polypeptide (Marrakchi et al., 2002).

Fatty acid synthase represents a valuable target for antimicrobial drug discovery due to its essential role in bacterial physiology and the structural divergence between bacterial and

mammalian systems. This distinction provides an opportunity for the development of selective antibacterial agents with minimal impact on human cells (Yao & Rock, 2018).

Within the bacterial Type II FAS system, the enzyme enoyl-acyl carrier protein (ACP) reductase, commonly known as FabI, has emerged as a validated drug target for antimicrobial therapy (Yao & Rock, 2018). FabI catalyzes the reduction of the trans-2-enoyl-ACP double bond in the last step of the type II fatty acid biosynthesis elongation cycle. This step is critical for the elongation of fatty acid chains, which are necessary for bacterial membrane lipid synthesis (Payne et al., 2002).

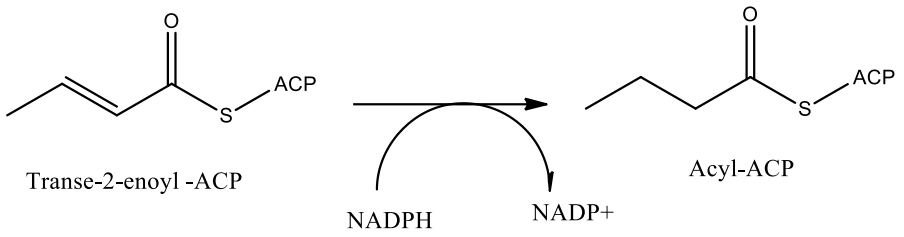

Figure 7: FabI-catalyzed final reduction step of fatty acid

There are several classes of FabI inhibitors, each targeting the enzyme's NADH-binding site or substrate interaction regions. Triclosan (**12**), which is a chlorinated bisphenol, is a broad-spectrum antibacterial agent that inhibits FabI. It forms a stable ternary complex with FabI and NADH, effectively locking the enzyme in an inactive state and halting fatty acid elongation. Despite its effectiveness, the widespread use of triclosan has led to resistance. Diazaborines are another class of FabI inhibitors that covalently bind to FabI. However, the inclusion of boron in their molecular structures makes them unsuitable for human use (Campbell & Cronan, 2001; Silverman et al., 2003). Additionally, isoniazid(**13**) a first-line antitubercular agent which inhibits fabI that binds to NAD^+ binding site and blocking enoyl-ACP reductase activity. This strategy

highlights the potential of NAD^+-competitive inhibition of FabI as a viable approach to overcome resistance mechanisms observed with traditional inhibitors (Zhang et al., 2006).

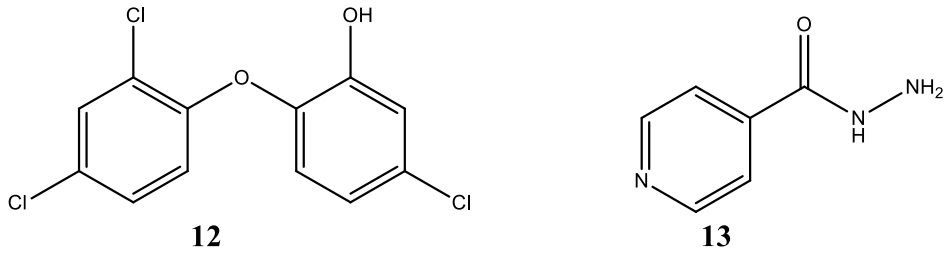

Figure 8: FabI inhibitors triclosan and isoniazid

1.3.3.2. ***Antifungal mechanism***

Similar to its antibacterial action, carvacrol and its derivatives disrupt the fungal cell membrane, causing cytoplasmic leakage. It also inhibits the synthesis of ergosterol, an essential component of the fungal cell membrane (Karadayı et al., 2020). Several antifungal drugs are available on the market that work by targeting the fungal cell membrane, either directly through binding to ergosterol or indirectly by inhibiting the biosynthesis of ergosterol. Polyene antifungals, such as nystatin and amphotericin B, bind to ergosterol in the fungal cell membrane to form pores or channels that allow essential ions to pass through and ultimately kill the cell. Amphotericin B is the most well-known polyene with a broad spectrum of action. However, its nephrotoxic effects limit its use (Serhan et al., 2014).

Azoles like fluconazole and ketoconazole are synthetic antifungals that inhibit lanosterol demethylase, the enzyme that catalyzes the transformation of lanosterol into ergosterol during ergosterol biosynthesis. Likewise, allylamines, such as terbinafine and naftifine, also act on an

enzyme in ergosterol biosynthesis called squalene epoxidase. Ciclopirox is a hydroxypyridone antifungal that targets the fungal cell by chelating metal ions, which disrupts cell membrane functions and impairs ergosterol biosynthesis (Niewerthl et al., 2002; Sanguinetti et al., 2005).

1.4. **Significance of the study**

Antibiotic resistance is a growing global health threat, highlighting the urgent need for new antimicrobial agents (Theuretzbacher, 2011). This study addresses this challenge by synthesizing and evaluating aminoalkyl derivatives of carvacrol, a natural phenolic compound with known antimicrobial properties (Wanda, 2023). Despite its broad activity, carvacrol's clinical use is limited by poor solubility, volatility, and low bioavailability (Santos et al., 2015). Chemical modification through aminoalkylation offers a strategic approach to enhance its pharmacokinetic and physicochemical properties.

The synthesized derivatives demonstrated potent antimicrobial activity, specifically against drug-resistant strains of bacteria and fungi. Additionally, *in silico* studies provided insights into their potential mechanisms of action and drug-likeness. This research not only advances the therapeutic potential of carvacrol derivatives but also contributes to the broader effort to combat antimicrobial resistance by identifying promising lead compounds for future development.

2. Objectives

2.1. General objective

To synthesize aminoalkyl derivatives of carvacrol, evaluate their *in vitro* antimicrobial activity and their potential mechanism of action through *in silico* studies.

2.2. Specific objectives

- To synthesize two aminoalkyl derivatives of carvacrol via a Mannich-type reaction involving the condensation of carvacrol with formaldehyde and a secondary amine (dimethylamine or piperidine).
- To characterize the synthesized aminoalkyl derivatives of carvacrol using spectroscopic techniques, specifically ^{1}H and ^{13}C-NMR.
- To assess the *in vitro* antibacterial and antifungal activities of the synthesized compounds against 26 bacterial and 4 fungal strains using disk diffusion and broth dilution methods.
- To perform *in silico* studies to evaluate the potential mechanisms of action and drug-likeness and ADMET properties of the synthesized compounds.

3. Materials and Methods

3.1. Materials

3.2. Chemicals and reagents

The following chemicals and reagents were used during the synthesis process: carvacrol, methanol (99.9%), ethanol (99.9%), formaldehyde (37%), chloroform (99.8%), anhydrous sodium sulfate, dimethyl amine, piperidine, and glacial acetic acid (all from Sigma-Aldrich Co., MO, USA). All the solvents and reagents are of analytical grade.

3.2.1. Instruments and apparatus

Silica gel analytical TLC plates (60 F254, 0.2 mm thick, Merck KGaA, Darmstadt, Germany) was used for chromatographic purposes. The TLC chromatograms were visualized using a UV-Visible Spectrophotometer (Evlution 60S). Refrigerator – for storing the mixture overnight.

Various equipment were used for the synthesis and antimicrobial testing, including an incubator (Model 100-800, Memmert), autoclave, biosafety cabinet (Biostar Model 50/60), vortex (Fisher Brand), water bath, inoculating loops, electrical weighing balance, magnetic stirrer, cavate, test tubes, pipette tips, pipette filler, micro-pipette (10-200 µl), microtiter plates, capillary tubes, and measuring cylinder.

NMR spectra were recorded using 400 MHz for ^{1}H and 100 MHz for ^{13}C on a Bruker Avance DMX400 FT-NMR spectrometer (Bruker, Billerica, 18 Massachusetts, and USA), tetramethyl silane (TMS) as internal standard and $CDCl_3$ was used as solvent.

3.2.2. Media, microbial strains, and Standard drugs

Media preparation involved the use of nutrient agar (NA), Mueller-Hinton broth (MHB), Sabouraud dextrose agar (SDA) and Sabouraud dextrose broth (SDB). For the antibacterial tests,

ciprofloxacin was used as the positive control, while 1% dimethyl sulfoxide (DMSO) served as the negative control. For antifungal tests, griseofulvin was used as the reference standard.

The *in vitro* antibacterial activity of the synthesized compounds were determined against the following Gram-positive strains: *Bacillus pumilus* 82, *Bacillus subtilis ATCC 6633, Staphylococcus, aureus* MDR10, *S.aureus MDR 1*, S.aureus MDR 2** and The Gram-negative bacteria were *E.coli NCTC 5933, E.coli K88, E.coli NCTC 7360, E.coli LT37, E.coli 872, E.coli ROW 7/12, E.coli 3:37C, E.coli CD/99/1, Salmonella typhi Ty2, Salmonella enterica TD 01, Shigella dysentery 8, Shigella soneii 1, Shigella boydii D13629, Shigella flexneri Type 6, Vibrio cholerae NCTC 4693, Vibrio cholerae NCTC5596, Vibrio cholerae NCTC 10732, Vibrio cholerae NCTC 11501, E.coli HB101*, E.coli C600*, Pseudomonas aeruginosa MDR 1*.* All bacterial strains were procured from the Department of Technology at Jadavpur University, the Central Drugs Laboratory in Kolkata, and the Institute of Microbial Technology in Chandigarh, India. The purity of the strains was confirmed by standard microbiological, cultural, and biochemical testing before their sensitivity to the test samples was assessed.

Similarly, antifungal activity was evaluated against the following fungal strains: *Candida albicans ATCC 10231, Aspergillus niger ATCC 6275, Penicillium notatum ATCC 11625,* and *Penicillium funiculosum NCTC 287.* All fungal strains were procured from the Central Drugs Laboratory in Kolkata and the Institute of Microbial Technology in Chandigarh, India.

3.3. **Methods**

3.3.1. **Synthesis of aminoalkyl derivatives of carvacrol (14 and 15)**

3.3.1.1. ***4-((Dimethylamino) methyl)-5-isopropyl-2-methylphenol (14)***

The general procedure for the synthesis of compound **14** was as follows: a solution of 0.75 ml (0.01 mol) of 37% aqueous formaldehyde in 10 ml of methanol was prepared in a 50 ml beaker, with five drops of acetic acid as a catalyst. Dimethylamine (0.66 ml, 0.01 mol) was added dropwise to a solution of formaldehyde and acetic acid to form an iminium intermediate, which was then added dropwise to a solution of carvacrol (1.5g, 0.01 mol) in methanol. The resulting mixture was thoroughly stirred and refluxed in a 250 ml Erlenmeyer flask for 28 hours at 100 °C. The reaction progress was monitored using TLC with a chloroform/ methanol (4:1) solvent system. After refluxing, the mixture was cooled to room temperature and poured into ice-cold water to precipitate the product, followed by overnight storage in a refrigerator to enhance precipitation. The resulting precipitate was filtered, washed with ethanol, and dried over anhydrous sodium sulfate (Na_2SO_4). Finally, the product is purified through recrystallization in ethanol to obtain the pure compound **14**.

3.3.1.2. ***5-Isopropyl-2-methyl-4-(piperidin-1-ylmethyl) phenol (15)***

Compound **15** was synthesized following a procedure similar to that used for compound **14**. A solution of 37% aqueous formaldehyde (0.75 mL, 0.01 mol) in 10 mL of methanol was prepared with five drops of acetic acid as a catalyst. Piperidine (1 mL, 0.01 mol) was added dropwise to form the iminium intermediate, which was then added dropwise to a methanolic solution of carvacrol (1.5 g, 0.01 mol). The reaction mixture was stirred and refluxed at 100°C for 20 hours, with reaction progress monitored by TLC. After refluxing, the mixture was cooled and poured into ice-cold water, then stored overnight in the refrigerator. The resulting precipitate was

filtered, washed with ethanol, dried over anhydrous Na_2SO_4, and recrystallized from ethanol to obtain pure compound **15**.

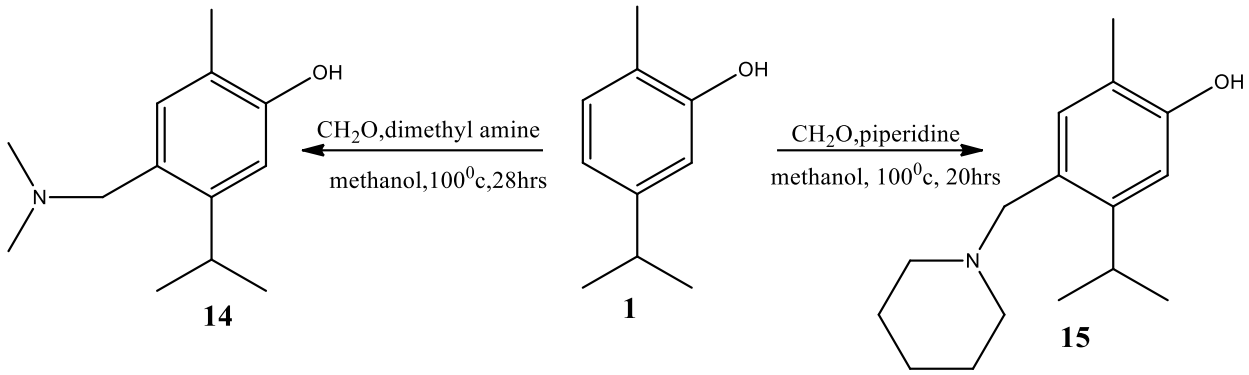

Scheme 1: Synthesis of aminoalkyl derivatives of carvacrol

3.3.2. **Spectroscopic analysis of the synthesized compounds**

The structures of compounds **14** and **15** were identified by analyzing their ^{1}H and ^{13}C-NMR spectra data. Chemical shifts are denoted in parts per million (*ppm)* and coupling constants (*J*) are expressed in *Hz*. Signal multiplicities are indicated as follows: *s* = singlet; *d* = doublet; *t* = triplet; *dd* = doublet of doublet; and *m* = multiplet.

3.3.3. ***In vitro*** **antibacterial and antifungal activity assay**

3.3.3.1. **Disc Diffusion Method**

The disc diffusion method was used to screen the *in vitro* antibacterial assay by comparing the zones of inhibition generated by the test samples with those of ciprofloxacin (Mitchell, J.K. and Carter, 2000). To investigate the synthesized compounds, 200 µg/mL of each of the test samples dissolved in 1% DMSO and ciprofloxacin dissolved in sterile distilled water were prepared. After that, sterile Petri dishes were filled with molten nutrient agar to create agar plates, which were then incubated at 37 °C for 24 hours to check for contamination. Once sterility was confirmed, the surface of each agar plate was uniformly inoculated with standardized bacterial

suspensions adjusted to 0.5 McFarland standards using a sterile cotton swab. Sterile filter paper discs (Whatman No. 1) with diameter 6 mm were then immersed in the test sample stock solution (200 µg/mL) and carefully placed on the surface of an agar plate. After being incubated for 24 hours at 37 °C, the diameter of the zones of inhibition in the petri dishes was measured in millimeters. A similar procedure was applied to pure ciprofloxacin, and the corresponding zone of inhibition was appropriately compared. 1% DMSO was used as a negative control (H & D, 2010).

For antifungal activity, a similar protocol was followed using Sabouraud Dextrose Agar (SDA) as the growth medium. The fungal pathogens were inoculated, and the plates were incubated for three days at room temperature. After incubation, the ZOI diameters were measured in millimeters. In this assay, griseofulvin was used as the standard for comparison.

3.3.3.2. **Broth Dilution Method**

The minimum inhibitory concentrations of the synthesized compounds were investigated by using broth dilution methods described by Jean B.etal (2015). Mueller–Hinton broth and Saborauds dextrose broth were used for bacterial and fungal growth, respectively. A broth with varying concentrations of the test sample ranging from 5 to 800 µg/mL for antibacterial activity testing and 50 to 2000 µg/mL for antifungal activity testing was made. 1% DMSO was used to dissolve the synthesized compounds. Furthermore, a growth control (nutrient broth with DMSO and inoculum, without antimicrobial agents) was included to confirm microbial viability, while a sterility control (nutrient broth with DMSO, without inoculum or antimicrobials) was included to ensure the absence of contamination. Each test and control well was incubated at 37 °C for 24 hours for bacteria and at 25 °C for three days for fungi. The MIC was identified as the lowest

concentration that inhibited visible growth, indicated by the absence of turbidity in the wells (V et al., 2023).

3.3.4. ***In silico*** **studies**

3.3.4.1. **Molecular docking study**

Molecular docking studies were performed with Maestro v13.5 of the Schrödinger 2023-1 Suite to determine the possible interaction of the synthesized compounds with the enoyl-acyl carrier protein reductase enzyme FabI, a key target in the fatty acid biosynthesis pathway in bacteria. The crystal structure of FabI of *E. coli* (PDB ID: 1C14), with a resolution of 2.00 Å, was obtained from the Protein Data Bank (PDB) and used for docking studies to assess the potential of the synthesized compounds as FabI inhibitors.

3.3.4.1.1. **Protein preparation**

The molecular docking procedure first involved preparing the FabI (PDB ID: 1C14) 3D structure using the Protein Preparation Wizard in Maestro. As part of the preparation, unnecessary components such as water molecules were removed so they would not affect ligand binding. Next, hydrogen atoms were added to the structure, correcting errors such as absent side chains, allocating appropriate bond ordering, correcting charges and atom types, and filling in missing side chains and loops. The Optimized Potentials for Liquid Simulations 4 (OPLS4) force field was applied for energy minimization to optimize molecular geometry and reduce steric clashes (Sastry et al., 2013).

3.3.4.1.2. **Ligand preparation**

Ligand preparation was performed using Schrödinger's LigPrep module. Structures were drawn in ChemDraw ultar12.0 and imported into LigPrep for conversion from 2D to 3D, with hydrogen

addition, computing correct partial charges, optimizing the structures, and achieving the appropriate protonation states at physiological pH 7.0 ± 2.0 by using Epik (Schrödinger, 2023). LigPrep also generated relevant ionization states, tautomers, and ring conformations for docking studies.

3.3.4.1.3. **Receptor Grid Generation**

Maestro v13.5's Grid Generation module was used to create the receptor. The grid was a cubic box, centered on the active site originally occupied by the co-crystallized ligand, which was excluded during the process. This approach ensured that new compounds could be docked precisely at the same binding site. The setup was specifically designed to facilitate the docking studies of amino alkyl carvacrol derivatives, allowing evaluation of their potential interactions within the defined binding pocket.

3.3.4.1.4. **Ligand docking**

Using the Glide tool in Maestro, molecular docking simulations were performed under extra precision (XP) modes. Ligands were docked into the FabI active site. The XP mode applied tighter scoring functions and constraints for improved accuracy. The Van der Waals scaling factor and partial charge cut-off for ligand atoms were adjusted to 0.80 and 0.15, respectively. Docking scores were used to estimate binding affinities by evaluating key interactions, such as hydrogen bonds, electrostatic, and hydrophobic interactions. To ensure reliability, redocking was performed by reintroducing the co-crystallized ligand into the active site of FabI and evaluating its binding affinity.

3.3.4.2. **Drug-likeness, Pharmacokinetics, and Toxicity Studies**

The drug-likeness, pharmacokinetics, and toxicity profiles of the synthesized compounds were predicted using the online ADMETlab 3.0 software. Initially, the 2D structures of the compounds

were drawn using ChemDraw Ultra 12.0, and their corresponding SMILES strings representations were generated for each compound. These SMILES were then pasted into the input field of the ADMETlab 3.0 web server to predict the absorption, distribution, metabolism, excretion, and toxicity (ADMET) profiles as well as drug-likeness.

4. Results and Discussion

In this study, aminoalkyl derivatives of carvacrol were successfully synthesized by carrying out a Mannich-type reaction. In this process, carvacrol was reacted with formaldehyde and two different secondary amines—dimethylamine and piperidine. This reaction involved the formation of an aminoalkyl group attached to the aromatic ring of carvacrol, resulting in the corresponding aminoalkylated products (**14** and **15**).

4.1. Synthesis of aminoalkyl derivatives of carvacrol (14 and 15)

4.1.1. 4-((Dimethylamino)methyl)-5-isopropyl-2-methylphenol (14)

Compound **14** was synthesized through a one-pot Mannich-type reaction, involving a three-component condensation of carvacrol, formaldehyde, and dimethylamine in the presence of an acid catalyst. The physical property of compound **14** is summarized in Table 1. The reaction occurs through a stepwise mechanism. Initially, glacial acetic acid enhances the electrophilicity of the carbonyl carbon in formaldehyde. This is followed by a nucleophilic addition of dimethylamine to formaldehyde, resulting in the elimination of water and the formation of an iminium ion intermediate. Subsequently, the formed iminium ion undergoes electrophilic aromatic substitution with the electron-rich aromatic ring of carvacrol, preferentially at the para position relative to the hydroxyl group. This sequence ultimately leads to the formation of compound **14**. The reaction mechanism is depicted in Schemes 2 and 3.

Table 1: Physical properties of the compounds **14** and **15**

Compound	Molecular Formula	Predicted MW(g/mol)	Physical State	Color	% Yield	Rf value
14	$C_{13}H_{21}NO$	207.31	Crystal	Colorless	85	0.45
15	$C_{16}H_{25}NO$	247.19	Crystal	Colorless	66	0.55

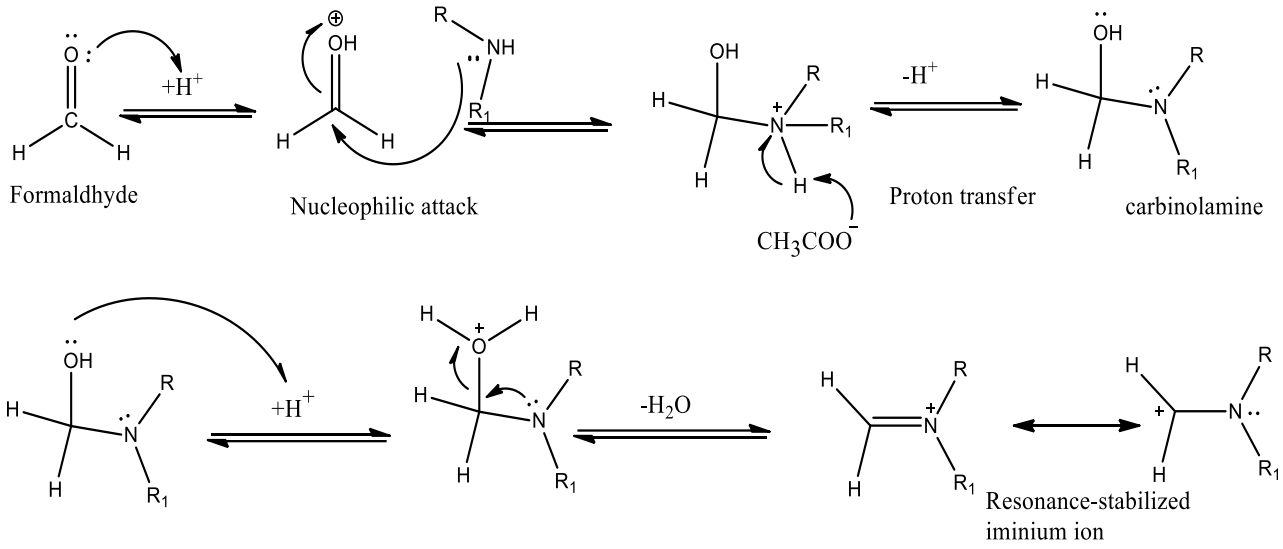

Scheme 2: Protonation of formaldehyde and formation of iminium ion

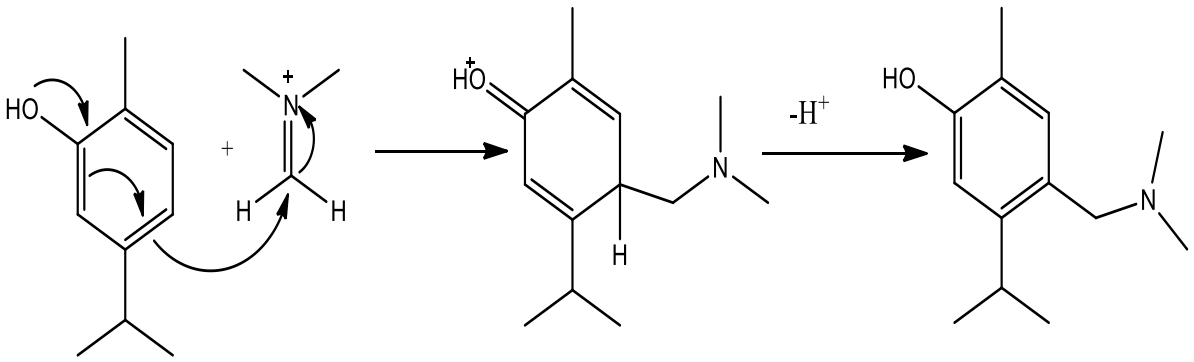

Scheme 3: Electrophilic aromatic substitution of compound **14**

4.1.2. **5-Isopropyl-2-methyl-4-(piperidin-1-ylmethyl) phenol (15)**

Using the same synthetic method described for compound **14**, compound **15** was synthesized through a Mannich-type reaction. In this reaction, piperidine was used as a substitute for dimethylamine, resulting in the successful formation of the compound **15**. The reaction mechanism closely resembles that of compound **14** and is illustrated in Schemes 2 and 4.

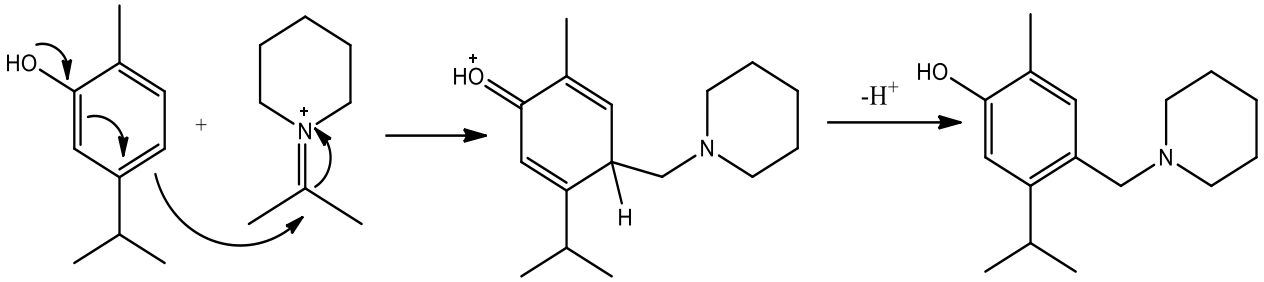

Scheme 4**:** Electrophilic aromatic substitution of compound **15**

4.2. **Structural confirmation of synthesized compounds 14 and 15**

The structures of compounds **14** and **15** were determined using ^{1}H-NMR and ^{13}C-NMR spectral data.

4.2.1. **4-((Dimethylamino)methyl)-5-isopropyl-2-methylphenol (14)**

The ^{1}H-NMR spectrum of compound **14** displayed two aromatic proton signals, assigned to H-6 (δ 6.56, ArH, *s*) and H-3 (δ 6.99, ArH, *s*), indicating that one of the aromatic protons in carvacrol was replaced by an aminoalkyl group. This confirms that the reaction occurred on the aromatic ring through substitution of one proton. Furthermore, a signal at δ 3.38 (2H, *s*) indicated the presence of a methylene group attached to a nitrogen atom, suggesting the formation of an aminoalkyl group in compound **14** (Appendix 1).

The ^{13}C-NMR confirmed the presence of a total of 13 carbon atoms in compound **14**. These included four quaternary carbons, five methyls (5xCH_3), three methines (3xCH), and one methylene (CH_2). The methylene carbon linking the aromatic ring to the dimethylamino group appeared at δC 60.26 ppm. The ^{1}H- NMR spectrum, combined with the ^{13}C- NMR data, confirms the proposed structure of 4-((dimethylamino) methyl)-5-isopropyl-2-methylphenol. The chemical shifts of all other protons and carbons in compound **14** are detailed in the Table 2.

4.2.2. **5-Isopropyl-2-methyl-4-(piperidin-1-ylmethyl) phenol (15)**

The ^{1}H-NMR spectra of compound **15** showed two aromatic protons, identified as H-6 (δ 6.72, 1H, *s*) and H-3 (δ 7.15, 1H, *s*). Additionally, one aromatic proton in carvacrol, which originally contained three aromatic protons, was replaced by an alkyl group. A singlet at δ of 3.75 ppm corresponded to the methylene (-CH_2-) group at position 10, linking the aromatic ring to the piperidine moiety, while signals at δ of 2.62, 1.47, and 1.66 ppm corresponded to protons at positions 2'and 6', 3' and 5', and 4', respectively, within the piperidine ring.

The ^{13}C-NMR confirmed the presence of a total of 16 carbon atoms in compound **15**. These included four quaternary carbons, three methyl carbons (3xCH_3), three methine carbons (3xCH), and six methylene carbons (CH_2). The methylene carbon linking the aromatic ring to the piperidine group was found at δ C 58.66 ppm, and the methylene carbons of the piperidine ring were observed at δ C 25.1, 26.73, and 55.53 ppm. Based on the combined ^{1}H and ^{13}C-NMR spectral data, compound **15** was identified as 5-isopropyl-2-methyl-4-(piperidin-1-ylmethyl) phenol. The remaining chemical shifts for both protons and carbons are provided in the Table 2.

Table 2: 1H and 13C-NMR spectral data of synthesized compounds

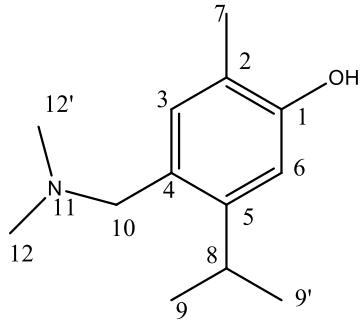

Compound **14**

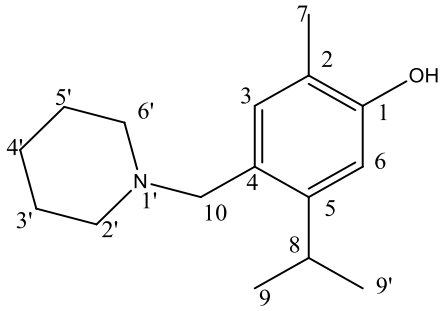

Compound **15**

Position	δ H (ppm)	δ C (ppm)	Position	δ H (ppm)	δ C (ppm)
1		153.93	1		153.30
2		121.09	2		128.51
3	6.99 (ArH, s)	133.44	3	7.15 (ArH, *s*)	133.86
4		126.42	4		129.53
5		147.01	5		138.08
6	6.56(ArH, s)	111.89	6	6.72 (ArH, *s*)	120.43
7	2.13(3H, *s*)	15.48	7	2.25(3H,*s*)	20.34
8	3.21(1H,*m*)	28.26	8	3.17 (1H, *m*):	28.25
9,9'	1.1(3H,3H,*d*, J = 8 Hz)	23.99	9,9'	1.26 (3H.3H, *d*, J = 8 Hz)	23.76
10	3.38(2H,*s*)	60.25	10	3.75(2H,s)	58.66
12,12'	2.25(3H,3H,*s*)	45.30	2', 6'	2.62(4H,*t*)	55.53
			3', 5'	1.66(4H,*m*)	26.73
			4'	1.47 (2H,*m*)	25.1

4.3. **Antimicrobial activity of compound 14 and 15**

4.3.1. **Antibacterial activity**

The antibacterial activity of compounds **14** and **15** was evaluated against 26 bacterial strains, comprising both Gram-negative and Gram-positive species. Two complementary methods were employed for this assessment: the disc diffusion assay, which measures the ZOIs caused by the compounds at a concentration of 200 µg/mL, and the broth dilution method, which determines the MIC necessary to inhibit bacterial growth. Ciprofloxacin, a well-established broad-spectrum antibiotic, was included in the study as a positive control.

Compounds **14** and **15** demonstrated comparable antibacterial activity against a broad range of bacterial strains, with ZOIs ranging from 6 to 16 mm and MICs ranging from 25 µg/mL to 400 µg/mL (Table 3). Compound **15** consistently exhibited greater antibacterial potency than compound **14**. This enhanced activity was evident from the larger zones of inhibition observed in the disc diffusion assay and the lower MIC values recorded in the broth dilution tests. For instance, compound **15** showed strong antibacterial activity against several clinically important pathogens, including *E. coli* (ZOI=12.5-16mm; MIC=25-100 µg/mL), *S. enterica* (ZOI=13.5mm; MIC=100 µg/mL), *various Shigella* species (ZOI=12.5-13mm; MIC=100 µg/mL), *Vibrio cholera* (ZOI=15.5-16mm; MIC=25 µg/mL), *S. aureus* (ZOI=9.5-13mm; MIC=50-400 µg/mL), and *P. aeruginosa* (ZOI=10mm; MIC=400 µg/mL). However, neither compound exhibited activity against *Bacillus pumilus* 82 (ZOI=6mm; MIC=NA) or *Bacillus subtilis* ATCC 6633 (ZOI=6mm; MIC=NA), as shown in Table 3.

Among the tested strains, both compounds were particularly effective against multiple *E. coli* isolates, a major causative agent of urinary tract infections, gastroenteritis, renal failure, and sepsis(Nataro & Kaper, 1998). For instance, compound **15** inhibited the growth of *E. coli* strains, with ZOI reaching up to 16.0 mm in diameter and exhibited MIC values as low as 25 µg/mL against these strains, indicating strong antibacterial efficacy. This result is particularly crucial as *E. coli* is one of the most prevalent bacteria that have been shown to have developed multi-drug resistance to many of the currently available antibiotics (Sader et al., 2002). Both compounds also exhibited moderate activity against *Salmonella* and *Shigella* strains, with zones of inhibition ranging from 11.5 to 13.5 mm and higher MIC values between 100–200 µg/mL, indicating less effectiveness against these more virulent pathogens. Compound **15** showed the weakest activity against *S. aureus* MDR1 and MDR2, with MIC values of 400 µg/mL. However, both compounds

displayed strong activity against *S. aureus* MDR10, with an MIC of 50 µg/mL. These findings suggest that while the compounds have some potential, they may not be sufficiently potent to effectively treat serious Gram-positive multidrug-resistant infections.

Vibrio cholerae is one of the most dangerous bacterial pathogens, commonly associated with severe diarrheal diseases in both humans and animals. In its acute form, cholera can lead to hypovolemia, potentially resulting in shock and death if left untreated (Chowdhury et al., 2022). In this study, both compounds **14** and **15** exhibited strong antibacterial activity against *V. cholerae*, with ZOIs ranging from 14 to 16 mm and MICs ranging from 25 to 50 µg/mL. These findings suggest that *Vibrio* species are particularly susceptible to the synthesized compounds.

In general, Gram-positive bacteria showed greater resistance to the compounds **14** and **15** compared to Gram-negative strains. Particularly, compound **15** demonstrated high activities against Gram-negative bacteria such as *E. coli* and *V. cholerae*.

Table 3: Zone of inhibition and minimum inhibitory concentration of the compound 14 and 15 against the tested bacterial strains

Name of Bacteria	Zone of inhibition in mm (200 µg/ml)			MIC (µg/ml)	
	Compound **14**	Compound **15**	Ciprofloxacin	Compound **14**	Compound **15**
E.coli NCTC 5933	13.0	15.0	16.0	50	25
E.coli K88	13.5	14.5	17.0	50	25
E.coli NCTC 7360	14.0	15.0	17.0	50	25
E.coli LT37	13.5	15.5	16.0	50	25
E.coli 872	14.0	15.0	16.0	50	25
E.coli ROW 7/12	14.0	15.5	16.5	50	25

E.coli 3:37C	14.5	16.0	16.5	50	25
E.coli CD/99/1	14.0	15.5	17.0	50	25
*E.coli HB101**	12.0	12.5	14.0	200	100
*E.coli C600**	11.5	13.0	13.5	200	100
Salmonella typhi Ty2	13.5	13.5	16.0	100	100
Salmonella enterica TD 01	13.5	13.5	19.0	100	100
Shigella dysentery 8	11.5	12.0	20.0	200	100
Shigella soneii 1	13.0	12.5	19.5	200	100
Shigella boydii D13629	12.0	12.0	20.0	200	100
Shigella flexneri Type 6	12.0	13.0	20.5	200	100
Staphylococcus aureus MDR10	13.5	13.0	18.0	50	50
*S.aureus MDR 1**	10.0	9.5	11.5	200	400
*S.aureus MDR 2**	11.5	10.0	12.0	200	400
Bacillus pumilus 82	6.0	6.0	19.0	NA	NA
Bacillus subtilis ATCC 6633	6.0	6.0	18.0	NA	NA
Vibrio cholerae NCTC 4693	14.0	15.5	17.5	50	25
Vibrio cholerae NCTC5596	14.5	16.0	18.5	50	25
Vibrio cholerae NCTC 10732	14.5	16.0	19.0	50	25
Vibrio cholerae NCTC 11501	14.5	15.5	18.5	50	25
*Pseudomonas aeruginosa MDR 1**	10.5	10.0	12.5	100	400

NA; no activity

4.3.2. **Antifungal activity**

Both synthesized compounds demonstrated antifungal activity against four fungal strains, with zones of inhibition ranging from 10.5 to 14.5 mm and MIC values between 200 and 800 µg/mL as summarized in Table 4. Overall, compound **15** exhibited stronger antifungal activity than compound **14** across all tested strains. Among the fungi evaluated, *Candida albicans* ATCC 10231 (ZOI= 14.5mm and MIC= 200 µg/mL) and *Penicillium funiculosum* NCTC 287 (ZOI=

13.5mm and MIC= 200) were the most susceptible to compound **15**, showing the largest zone of inhibition (14.5 mm) and the lowest MIC (200 µg/mL), indicating notable antifungal potency. A comparative assessment of both compounds revealed differences in activity levels against the tested fungal strains (Table 4).

Table 4: Zone of inhibition and minimum inhibitory concentration of the compound 14 and 15 against the tested fungal species

Name of Fungi	Zone of inhibition in mm(2000µg/ml)			MIC(µg/ml)	
	Compound	Compound	Griseofulvin	Compound	Compound
Candida albicans ATCC 10231	12.0	14.5	16.0	400	200
Aspergillus niger ATCC 6275	11.0	14.0	15.0	800	400
Penicillium notatum ATCC 11625	11.0	13.0	13.5	800	400
Penicillium funiculosum NCTC 287	10.5	13.5	14.0	800	200

4.4. *In silico* analysis

4.4.1. Molecular docking analysis

Molecular docking analysis of the synthesized compounds **14** and **15** was conducted against the *E. coli* FabI enzyme (PDB ID: 1C14) to assess their binding affinities, using triclosan as the reference ligand.

Molecular docking analysis of compound **14** with *E. coli* enoyl-acyl carrier protein reductase (FabI; PDB ID: 1C14), a key enzyme in bacterial fatty acid biosynthesis, revealed promising interactions within the enzyme's active site. Compound **14** achieved a docking score of –5.677 kcal/mol and glide energy of –25.140 kcal/mol, indicating favorable binding affinity. As shown in the 2D and 3D interaction diagrams (Figures 9 and 10), the compound fits well into the catalytic pocket of FabI, forming several stabilizing interactions.

Particularly, compound **14** forms a hydrogen bond with the critical residue Lys163 and polar interactions with Ser145 and Thr194, residues commonly associated with the enzyme's active

site. These interactions help anchor the compound in a favorable orientation, potentially mimicking the natural substrate or interfering with NADH binding. In addition to hydrogen and polar interactions, compound **14** engages in significant hydrophobic interactions with lipophilic regions of the binding pocket, such as Leu144, Met159, Tyr156, Phe203, Ile200, Ala197, Ala189, Met206, Ile192, Pro191, and Ile20 and also forms a π–cation stacking interaction with Tyr146, further stabilizing its conformation. Together, these interactions contribute to strong binding affinity and suggest that compound **14** may inhibit FabI by occupying the NADH binding site or blocking substrate access. Overall, the docking results support the potential of compound **14** as an effective FabI-targeting antimicrobial agent against *E. coli*.

Table 5: Docking scores and glide energy of synthesized compounds

Ligand	**Docking score (kcal/mol)**	**Glide energy (kcal/mol)**	**Key Interactions**	
			H-bonds	None H-bonds
Compound **14**	-5.677	-25.140	Lys163	Tyr146, Ser145, Thr194
Compound **15**	-4.976	-29.372	Gly93	Lys 163, HIE90, Ser91, Ser145, Thr194
Triclosan	-7.194	-35.771	Thr194	Lys163, Tyr146

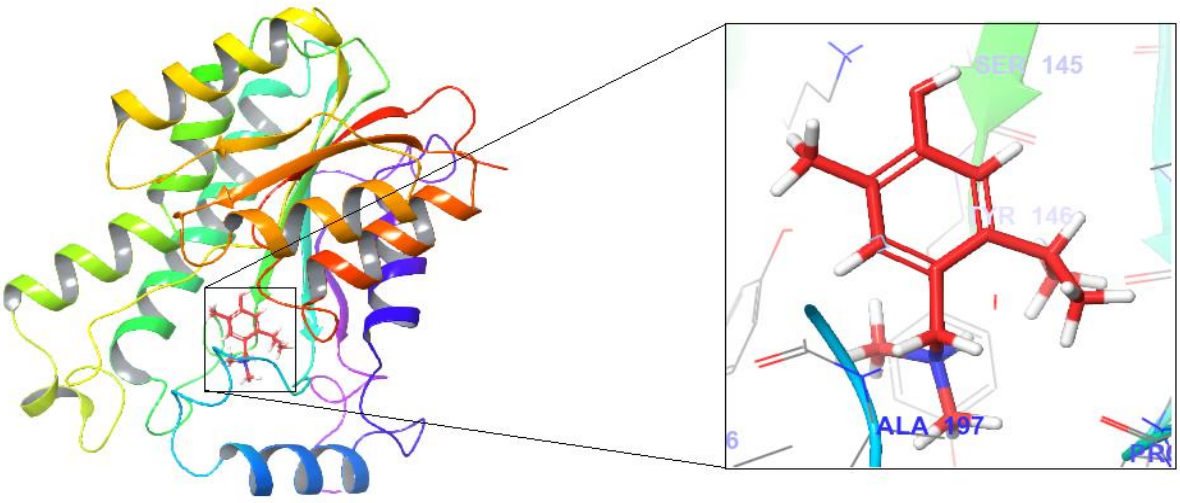

Figure 9: 3D interaction between compound **14** and *E. coli* FabI (PDB ID: 1C14)

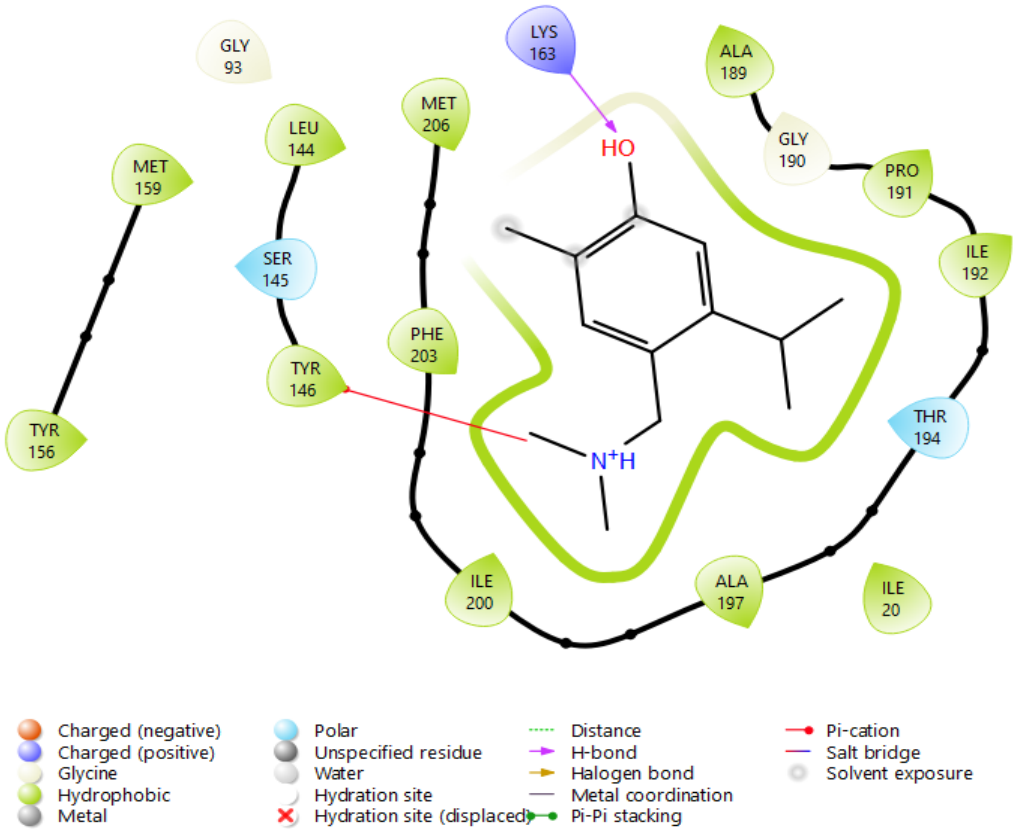

Figure 10: 2D interaction between compound **14** and *E. coli* FabI (PDB ID: 1C14)

The molecular docking analysis of compound **15** with *E. coli* FabI (PDB ID: 1C14) revealed favorable binding interactions within the enzyme's active site, with a docking score of –4.976 kcal/mol and glide energy of –29.372 kcal/mol (Table 5). As shown in the 2D and 3D interaction diagrams (Figures 11 and 12), compound **15** fits well into the catalytic pocket, forming several key interactions with surrounding amino acid residues. These include a hydrogen bond with Gly93 and polar interactions with critical residues such as Hie90, Ser91, Ser145, and Thr194, which likely contribute to the stability and specificity of the binding.

Additionally, hydrophobic interactions between the non-polar regions of compound **15** and the lipophilic residues in the binding site further enhance its affinity for FabI. The presence of aromatic or planar groups in compound **15** also enables π–π stacking interactions with Lys163,

which are often involved in stabilizing inhibitors within the active site of FabI. This combination of hydrogen bonding, hydrophobic interactions, and π–π stacking suggests that compound **15** effectively occupies the enzyme's active region, potentially interfering with NADH cofactor binding or substrate access. Overall, the docking profile of compound **15** indicates moderate binding potential to FabI, supporting its promise as a lead compound for the development of new antibacterial agents targeting *E. coli* FabI.

To validate the reliability of the docking protocol, triclosan which is known inhibitor of *E. coli* FabI—was redocked into the enzyme's active site under the same conditions used for the synthesized compounds. The redocking yielded a docking score of –7.194 kcal/mol, confirming the validity of the docking approach.

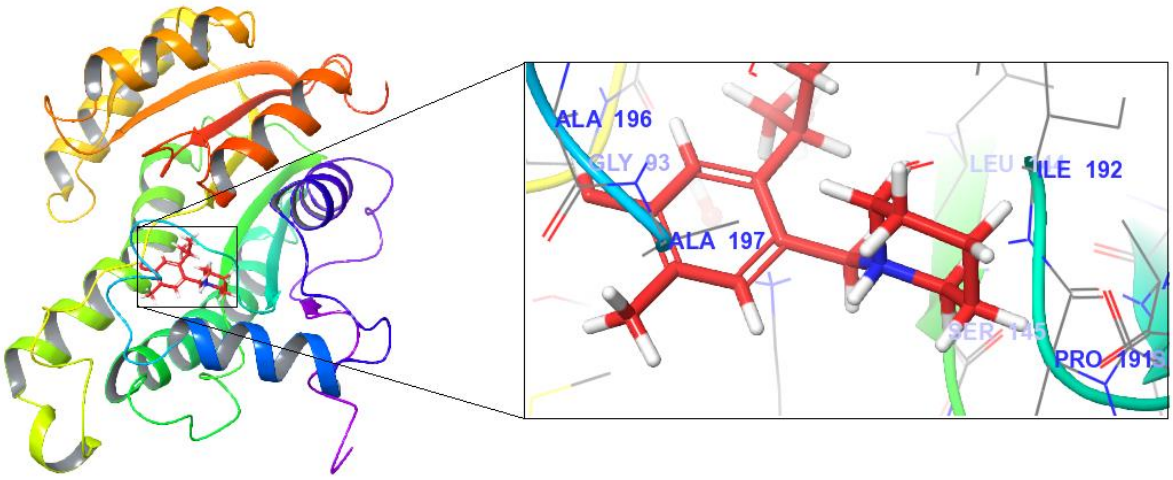

Figure 11: 3D interaction between compound **15** and *E. coli* FabI (PDB ID: 1C14)

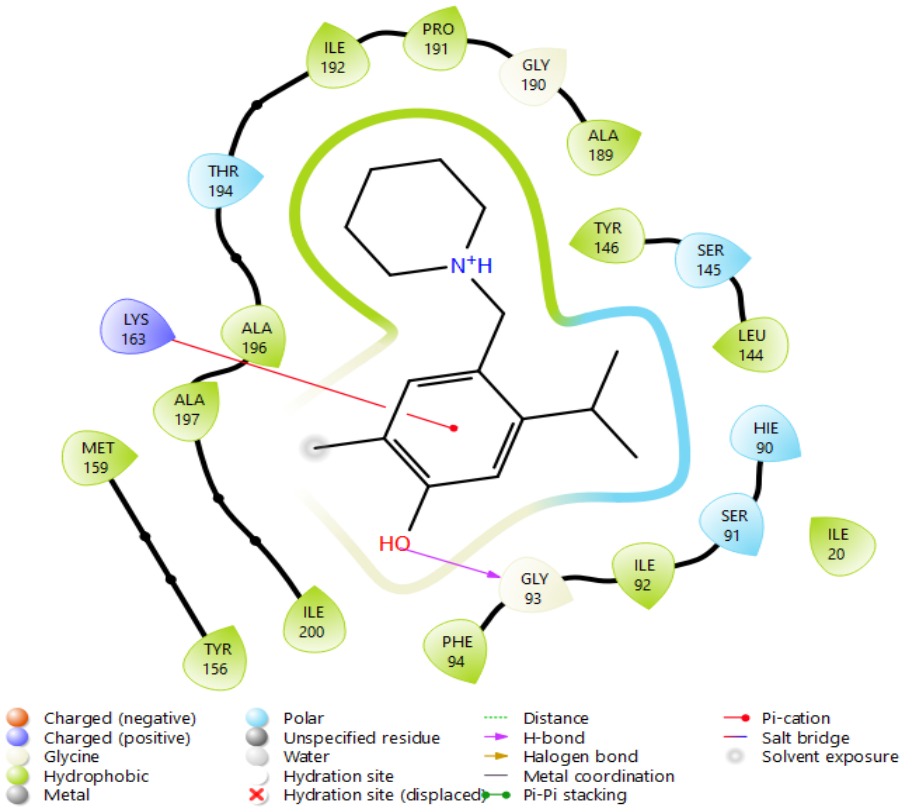

Figure 12: 2D interaction between compound **15** and *E. coli* FabI (PDB ID: 1C14)

4.4.2. **Drug-Likeness, and ADMET properties**

4.4.2.1. **Drug-Likeness**

Physicochemical and medicinal chemistry properties are essential for determining the drug-likeness of compounds. Early prediction of these parameters, such as through Lipinski's Rule of Five, can significantly increase the likelihood of success in lead optimization. Key factors like solubility, lipophilicity, hydrogen bonding capacity, molecular flexibility, and synthetic accessibility help predict oral bioavailability, membrane permeability, and overall pharmacokinetic behavior (Lipinski et al., 2001; Serdaroğlu, 2023). Using ADMET Lab 3.0, the physicochemical and drug-likeness properties of synthesized compounds **14** and **15** were analyzed and presented in Table 6 alongside triclosan for comparison. Both compounds showed

values within acceptable ranges. Compound **14** demonstrated superb aqueous solubility and moderate lipophilicity, reflecting excellent physicochemical properties. Compound **15**, although slightly more lipophilic with higher LogP and LogD values, still falls within acceptable limits. While increased lipophilicity may enhance membrane permeability, it can also lead to reduced solubility, higher toxicity, and faster metabolic clearance (Naylor et al., 2018). Both compounds satisfied Lipinski's criteria and showed favorable values for hydrogen bonding, molecular flexibility, and topological polar surface area (TPSA = 23.47 $Å^2$), supporting good permeability (Babalola & Igie, 2022). High QED scores indicate strong drug-likeness, and low synthetic accessibility (SA) scores suggest both compounds are practical to synthesize, making them promising candidates for further development.

When compared to triclosan, a known antimicrobial agent, both compounds showed comparable or better solubility and synthetic accessibility**,** while maintaining acceptable ranges in lipophilicity and hydrogen bonding. Triclosan's higher LogP and lower solubility suggest it is less water-soluble and more lipophilic than both synthesized compounds.

Table 6: Physicochemical, and drug-likeness properties of the synthesized compounds

Parameters	Compound **14**	Compound **15**	Triclosan	Reference Range	Interpretation
nHA (H-bond acceptors)	2	1	2	0–12	Both are within acceptable range.
nHD (H-bond donors)	1	1	1	0–7	Indicates acceptable H-bonding for oral bioavailability.
nRot (rotatable bonds)	3	3	2	0–11	Suggests moderate molecular flexibility.
TPSA ($Å^2$) (topological polar surface area)	23.47	23.47	29.46	0–140	Low TPSA, favorable for membrane permeability and oral absorption.
LogS (solubility)	-2.535	-3.469	-4.555	-4 to 0.5	Compound 14 has better aqueous solubility; both are within range.
LogP (lipophilicity)	2.789	3.774	4.512	0–3	Compound 14 has moderate lipophilicity; compound 15 is slightly above the ideal.
LogD (distribution at pH 7.4)	2.36	3.234	3.494	1–3	Both compounds show good membrane permeability; compound 15 is near upper limit.
Lipinski's Rule of 5	Accepted	Accepted	Accepted	—	Indicates good oral drug-likeness.
QED (quantity estimate of drug-likeness)	0.823	0.878	0.829	>0.67	High QED scores indicate strong drug-like properties.
SA score (synthetic access)	2	2	1	≤6	Both are synthetically accessible.

4.2.2.2. ADMET Properties

In silico ADMET prediction models are widely used in drug design to support medicinal chemists in optimizing lead compounds. Using the ADMET Lab 3.0 online tool, the pharmacokinetic and toxicity profiles of compounds **14** and **15** were evaluated, with results summarized in Table 7 with triclosan included as a reference for comparison. The tool predicts critical parameters related to absorption, distribution, metabolism, elimination, and toxicity, including insights into blood-brain barrier (BBB) permeability, gastrointestinal absorption, P-glycoprotein (P-gp) interaction, and cytochromeP450 (C P450) enzyme inhibition (Fu et al., 2024).

Caco-2 cell permeability is commonly used to estimate human intestinal absorption, with values above -5.15 cm/s indicating good absorption potential. Both compounds exceeded this threshold, suggesting strong oral absorption. The Human Intestinal Absorption (HIA) model also predicted high absorption, with both compounds scoring below 0.01. Furthermore, neither compound is a substrate for P-gp, meaning they are unlikely to be actively effluxed from cells, which supports better intracellular retention and oral bioavailability (Lin & Yamazaki, 2003).

The volume of distribution (VDss) for compounds **14** and **15** was 0.454 and 0.617 L/kg, respectively well within the acceptable range of 0.04–20 L/kg. BBB permeability was favorable for compound **15** (0.66), suggesting effective penetration into the central nervous system. Compound **14**, however, showed a lower value (0.462), indicating limited BBB crossing. Both compounds showed no inhibitory activity against CYP1A2, CYP2C19, and CYP2C8 enzymes, implying a low risk of metabolic drug–drug interactions.

In terms of clearance, both compounds exhibited good elimination rates, although compound **14** had a slightly prolonged half-life of 0.964, exceeding the medium threshold (0.7), which may result in extended systemic exposure (Benet et al., 2002). Toxicity predictions revealed low hERG inhibition and minimal p53 activation, indicating low cardiotoxicity and genotoxicity. Additionally, compound **15** demonstrated a lower Ames mutagenicity score than compound **14**, suggesting a more favorable safety profile. Overall, these findings highlight the promising pharmacokinetic behavior and safety potential of both compounds, especially compound **15.**

Triclosan, used here as a reference antimicrobial, exhibited higher plasma protein binding, lower clearance, and a longer half-life, indicating greater systemic retention and reduced free drug availability. Additionally, triclosan showed higher BBB permeability and stronger hERG inhibition, suggesting higher CNS penetration and potential cardiotoxicity. These differences highlight the more balanced and safer pharmacokinetic profiles of compounds **14** and **15.**

Table 7: Prediction of ADMET properties of the synthesized compounds

Parameter	Compound **14**	Compound **15**	Triclosan	Recommended Range	Interpretation
Caco-2 permeability	-4.765	-4.725	-4.805	> -5.15	Good intestinal permeability predicted for both.
PPB (%plasma protein bound)	82.545%	86.3%	99.158%	< 90%	Acceptable plasma protein binding.
HIA (absorption)	0.0	0.0	0.0	0.0–0.1	Good human intestinal absorption predicted.
Pgp-substrate	0.055	0.018	0.004	0.0–0.1	Low risk of P-glycoprotein efflux; favorable for oral bioavailability.
VDss (L/kg)	0.454	0.617	-0.149	0.04–20	Moderate volume of distribution.
BBB permeability	0.462	0.66	0.967	0.5–0.7	Compound 15 may cross the blood-brain barrier; compound 14 is borderline.
CYP inhibition	All values < 0.1	All values < 0.1	All values < 0.1	0.0–0.1	Both compounds are unlikely to inhibit major CYP450 enzymes favorable.
Clearance (mL/min/kg)	13.946	9.668	6.416	≥ 5	Both have acceptable drug clearance rates.
Half-life (T½)	0.964	0.465	1.139	0.3–0.7 (medium)	Compound 15 shows moderate stability; compound 14 has a slightly longer half-life.
hERG inhibition (human ether-a-go-go related gene)	0.358	0.64	0.89	0.0–0.7	Within medium risk; compound 15 closer to upper bound.
Ames test	0.413	0.248	0.246	0.0–0.3	Compound 15 shows lower mutagenic potential than 14.
SR-p53 interaction (a tumor suppressor protein p53)	0.00	0.068	0.458	0.0–0.3	Low toxicity risk for both.

In summary, compound **14** demonstrates better aqueous solubility and lower lipophilicity, along with strong drug-likeness and moderate ADMET properties. In contrast, compound **15** exhibits higher lipophilicity, contributing to slightly enhanced membrane permeability and increased blood–brain barrier (BBB) permeability. However, this increased lipophilicity may also be associated with a slightly elevated risk of toxicity. Despite these differences, both compounds satisfy Lipinski's Rule of Five, have high QED scores indicating strong drug-like characteristics, and possess low synthetic accessibility scores, suggesting they are easy to synthesize. These attributes make both compounds promising candidates for further drug development, warranting additional *in vitro* and *in vivo* investigation.

5. Conclusion

In this study, two novel aminoalkyl derivatives of carvacrol, 4-((dimethylamino)methyl)-5-isopropyl-2-methylphenol **(14)** and 5-isopropyl-2-methyl-4-(piperidin-1-ylmethyl)phenol **(15)**, were synthesized using a Mannich-type reaction. Both compounds exhibited broad-spectrum antimicrobial activity, with compound **15** demonstrating superior antimicrobial activity. For instance, compound **15** showed stronger antibacterial activity against *E. coli* (MIC: 25 μg/mL) compared to compound **14** (MIC: 50 μg/mL), highlighting its superior potency and potential as a lead compound for treating infections such as urinary tract infections, gastroenteritis, and sepsis. Additionally, it displayed potent antifungal activity against *C. albicans* and *P. funiculosum* (MIC: 200 μg/mL). Molecular docking studies revealed that both derivatives interact favorably with the active site and may inhibit the *E. coli* FabI enzyme, which plays a critical role in fatty acid elongation essential for bacterial membrane synthesis. These findings support the potential of structural modifications of carvacrol to improve its antimicrobial profile.

6. Recommendations

Based on the observed broad-spectrum antimicrobial activity of the synthesized aminoalkyl derivatives of carvacrol, the following recommendations are proposed:

- Conduct cytotoxicity assays to determine the safety profile of these compounds, along with pharmacokinetic studies and in vivo efficacy assessments to validate their therapeutic potential.
- Synthesize and evaluate a wide range of aminoalkyl carvacrol derivatives for activity against bacterial and fungal strains.
- Explore the potential of these compounds to interact with other biologically relevant microbial targets, particularly DNA-related enzymes such as bacterial DNA gyrase and topoisomerases.
- Explore additional biological activities of the synthesized aminoalkyl derivatives of carvacrol, including antioxidant, anti-inflammatory, anticancer, antiviral, and antiparasitic effects, to broaden their potential pharmacological applications.

References

Alokam, R., Jeankumar, V. U., Sridevi, J. P., Matikonda, S. S., & Peddi, S. (2014). Identification and structure – activity relationship study of carvacrol derivatives as Mycobacterium tuberculosis chorismate mutase inhibitors. *Journal of Enzyme Inhibition and Medicinal Chemistry*, *6366*(4), 547–554.

Annunziato, G. (2019). Strategies to overcome antimicrobial resistance (AMR) making use of non-essential target inhibitors: A review. *International Journal of Molecular Sciences*, *20*(23).

Babalola, S., & Igie, N. (2022). of p -Nitrophenyl Hydrazones as Anti-in fl ammatory Compounds against COX-2 , 5-LOX , and H þ / K þ ATPaseMolecular Docking , Drug-Likeness Analysis , In Silico Pharmacokinetics , and Toxicity Studies. *Pharmaceut Fronts*, *4*, e250–e266.

Baranauskaite, J., Duman, G., Corapcioğlu, G., Baranauskas, A., Taralp, A., Ivanauskas, L., & Bernatoniene, J. (2018). Liposomal Incorporation to Improve Dissolution and Stability of Rosmarinic Acid and Carvacrol Extracted from Oregano (O. onites L.). *BioMed Research International*, *2018:61473*, 1–10.

Baser, K. H. C. (2008). Biological and Pharmacological Activities of Carvacrol and Carvacrol Bearing Essential Oils. *Curr Pharm Des.*, *14*(29), 3106–3119.

Bendre, R., Bagul, S., & Rajput, J. (2018). Natural Products Chemistry & Carvacrol : An Excellent Natural Pest Control Agent. *Nat Prod Chem Res*, *6*(6), 20–22.

Benet, L. Z., Hoener, B., & Francisco, S. (2002). C LINICAL. *Clin Pharmacol Ther*, *71*(3), 115–121.

Berhe, D. F., Beyene, G. T., Seyoum, B., Gebre, M., Haile, K., Tsegaye, M., Boltena, M. T., Tesema, E., Kibret, T. C., Biru, M., Siraj, D. S., Shirley, D., Howe, R., & Abdissa, A. (2021). Prevalence of antimicrobial resistance and its clinical implications in Ethiopia : a systematic review. *Antimicrobial Resistance & Infection Control*, *10*(1), 168.

Bhardwaj, R., Parihar, P., Yadav, K., Bardhan, N. B., & Komal, Y. (2018). Synthesis,

Characterization and Application of Mannich Base. *Galore International Journal of Applied Sciences and Humanities (Www.Gijash.Com)*, *2*(2), 19.

Bongomin, F. (2017). Global and Multi-National Prevalence of Fungal Diseases — Estimate Precision. *J Fungi (Basel)*, *3*(4), 57.

Cacciatore, I., Giulio, M. Di, Fornasari, E., Stefano, A. Di, Cerasa, S., Marinelli, L., Turkez, H., Campli, E. Di, & Di, S. (2015). Carvacrol Codrugs : A New Approach in the Antimicrobial Plan. *PLoS One*, *10*(4), 1–20.

Campbell, J. W., & Cronan, J. E. (2001). B ACTERIAL F ATTY A CID B IOSYNTHESIS : Targets for Antibacterial Drug Discovery. *Annu Rev Microbiol*, *55*, 305–332.

Chowdhury, F., Ross, A. G., Islam, T., & Mcmillan, N. A. J. (2022). Diagnosis , Management , and Future Control of Cholera. *Clin Microbiol Rev*, *35*(3), 1–23.

Denning, D. W. (2024). Global incidence and mortality of severe fungal disease. *Lancet Infect Dis*, *24*(7), e428–e438.

Frieri, M., Kumar, K., & Boutin, A. (2016). Antibiotic resistance. *Journal of Infection and Public Health*, *10*(4), 369–378.

Fu, L., Shi, S., Yi, J., Wang, N., He, Y., Wu, Z., Peng, J., Deng, Y., Wang, W., Wu, C., Lyu, A., Zeng, X., Zhao, W., Hou, T., & Cao, D. (2024). ADMETlab 3 . 0 : an updated comprehensive online ADMET prediction platform enhanced with broader coverage , impro v ed perf ormance , API functionality and decision support. *Nucleic Acids Research*, *52*(W1), 422–431.

Fu, L., Wan, M., Zhang, S., Gao, L., & Fang, W. (2020). Polymyxin B Loosens Lipopolysaccharide Bilayer but Stiffens Phospholipid Bilayer. *Biophysj*, *118*(1), 138–150.

Gnimatin, J. P., Weyori, E. W., Agossou, S. M., & Adokiya, M. N. (2022). Bacterial infections epidemiology and factors associated with multidrug resistance in the northern region of Ghana. *Scientific Reports*, *12:22069*, 1–12.

H, M. S. S., & D, H. P. (2010). Antimicrobial activity and phytochemical analysis of selected

Indian folk medicinal plants. *International Journal of Pharma Sciences and Research (IJPSR)*, *1*(10), 430–434.

Hao, Y., Li, J., & Shi, L. (2021). A Carvacrol-Rich Essential Oil Extracted From Oregano (Origanum vulgare “Hot & Spicy”) Exerts Potent Antibacterial Effects Against Staphylococcus aureus. *Frontiers in Microbiology*, *12:741861*(r), 1–13.

Herrera-calderon, O., Yepes-p, A. F., Quintero-saumeth, J., Rojas-armas, J. P., Palomino-pacheco, M., Ortiz-s, M., Edwin, C., Arroyo-acevedo, J. L., Figueroa-salvador, L., & Peña-rojas, G. (2020). Carvacrol : An In Silico Approach of a Candidate Drug on HER2 , PI3K α , mTOR , hER- α , PR , and EGFR Receptors in the Breast Cancer. *Evidence-Based Complementary and Alternative Medicine, 2020: 8830*.

Ikuta, K. S. et al. (2022). Global mortality associated with 33 bacterial pathogens in 2019 : a systematic analysis for the Global Burden of Disease Study 2019. *The Lancet*, *400*(10369), 2221–2248.

Karadayı, M., Yıldırım, V., & Güllüce, M. (2020). Antimicrobial Activity and Other Biological Properties of Oregano Essential Oil and Carvacrol 2 . Bioactivities of Oregano Essential Oil and Carvacrol. *Anatolian Journal of Biology*, *2*, 52–68.

Lazarević, J., Marković, A., Šmelcerović, A., Stojanović, G., Ciuffreda, P., & Santaniello, E. (2022). Carvacrol Derivatives as Antifungal Agents : Synthesis , Antimicrobial Activity and in Silico Studies on Carvacryl Esters. *Acta Chim Slov*, *69*(3), 571–583.

Lin, J. H., & Yamazaki, M. (2003). Role of P-Glycoprotein in Pharmacokinetics Clinical Implications. *Clin Pharmacokinet*, *42*(1), 59–98.

Lipinski, C. A., Lombardo, F., Dominy, B. W., & Feeney, P. J. (2001). Experimental and computational approaches to estimate solubility and permeability in drug discovery and development settings. *Adv Drug Deliv Rev*, *46*(1–3), 3–26.

Marinelli, L., Di, A., & Ivana, S. (2018). Carvacrol and its derivatives as antibacterial agents. *Phytochemistry Reviews*, *7*, 903–921.

Marrakchi, H., Zhang, Y., & Rock, C. O. (2002). Mechanistic diversity and regulation of Type II

fatty acid synthesis Bacterial Type II fatty acid synthesis. *Biochem Soc Trans*, *30*(Pt 6), 1050–1055.

Memar, M. Y., Raei, P., & Alizadeh, N. (2017). Carvacrol and thymol : strong antimicrobial agents against resistant isolates. *Reviews in Medical Microbiology*, *28*(2), 63–68.

Metrics, G. H. (2020). Global burden of 369 diseases and injuries in 204 countries and territories , 1990 – 2019 : a systematic analysis for the Global Burden of Disease Study 2019. *Lancet*, *396*(10258), 1204–1222.

Mitchell, J.K. and Carter, W. . (2000). Modeling Antimicrobial Activity of Clorox (R) Using an Agar-Diffusion Test: A New Twist on an Old Experiment. *Bioscene*, *26*(3), 9–13.

Mohammedi, Z. (2017). Carvacrol : An Update of Biological Activities and Mechanism of Action. *Open Access J Chem*, *1*(1), 53–62.

Nataro, J. P., & Kaper, J. B. (1998). Diarrheagenic Escherichia coli. *Clin Microbiol Rev*, *11*(1), 142–201.

Naylor, M. R., Ly, A. M., Handford, M. J., Ramos, D. P., Pye, C. R., Furukawa, A., Klein, V. G., Noland, R. P., Edmondson, Q., Turmon, A. C., Hewitt, W. M., Schwochert, J., Townsend, C. E., Kelly, C. N., Blanco, M., & Lokey, R. S. (2018). Aqueous Solubility Inversely Proportional to log [Research-article]. *Journal of Medicinal Chemistry*, *61*, 11169–11182.

Niewerthl, M., Schaller, M., Hube, H. C. K. B., & Candida, S. (2002). Mode of action of ciclopiroxolamine on Candida albicans. *Mycoses*, *68*(Suppl 1), 63–68.

Nikumbh, V. P., Mahulikar, P. P., & Methods, E. (2003). Eco-friendly Pest Management Using J.\t1onoterpenoids-III: Antibacterial Efficacy of Carvacrol Derivatives#. *Jo Urn Al of Scientifi c & Indu s Tri Al Research*, *62*(r), 1086–1089.

Oliveira, A. S. De, Llanes, L. C., Maria, I., Brighente, C., Nunes, R. J., Yunes, R. A., & Jr, N. M. (2016). New Sulfonamides Derived from Carvacrol : Compounds with High Antibacterial Activity against Resistant Staphylococcus aureus Strains. *Journal of Biosciences and Medicines*, *4*(7), 105–114.

Payne, D. J., Miller, W. H., Berry, V., Brosky, J., Burgess, W. J., Chen, E., DeWolf, W. E., Fosberry, A. P., Greenwood, R., Head, M. S., Heerding, D. A., Janson, C. A., Jaworski, D. D., Keller, P. M., Manley, P. J., Moore, T. D., Newlander, K. A., Pearson, S., Polizzi, B. J., … Huffman, W. F. (2002). Discovery of a novel and potent class of fabI-directed antibacterial agents. *Antimicrobial Agents and Chemotherapy*, *46*(10), 3118–3124.

Prashanth, T., Ranganatha, V. L., Ramu, R., Mandal, S. P., Mallikarjunaswamy, C., & Khanum, S. A. (2021). Synthesis , characterization , docking study and antimicrobial methyl)- 1 H - benzo [d] imidazol - 1 - yl] ethanone derivatives. *Journal of the Iranian Chemical Society*, *18*(10), 2741–2756.

Rad, M. S., Setzer, W. N., Iriti, M., Martorell, M., Varoni, E. M., & Salehi, B. (2018). Carvacrol and human health : A comprehensive review. *Phytother Res*, *32*(9), 1675–1687.

Sader, H. S., Jones, R. N., Silva, J. B., Sentry, T., Group, P., & America, L. (2002). Skin and soft tissue infections in Latin American medical centers : four-year assessment of the pathogen frequency and antimicrobial susceptibility patterns. *Diagn Microbiol Infect Dis*, *44*(3), 281–288.

Salam, A., Al-amin, Y., Salam, M. T., & Pawar, J. S. (2023). Antimicrobial Resistance : A Growing Serious Threat for Global. *Healthcare (Basel)*, *11*(13:1946).

Sanguinetti, M., Posteraro, B., Fiori, B., Ranno, S., Torelli, R., & Fadda, G. (2005). Mechanisms of Azole Resistance in Clinical Isolates of Candida glabrata Collected during a Hospital Survey of Antifungal Resistance. *Antimicrob Agents Chemother*, *49*(2), 668–679.

Santos, E. H., Kamimura, J. A., Hill, L. E., & Gomes, C. L. (2015). LWT - Food Science and Technology Characterization of carvacrol beta-cyclodextrin inclusion complexes as delivery systems for antibacterial and antioxidant applications. *LWT - Food Science and Technology*, *60*(1), 583–592.

Sartorius, B., Gray, A. P., Weaver, N. D., Aguilar, G. R., Swetschinski, L. R., Ikuta, K. S., Mestrovic, T., Chung, E., Wool, E. E., & Han, C. (2024). The burden of bacterial antimicrobial resistance in the WHO African region in 2019: a cross-country systematic analysis. *The Lancet Global Health*, *12*(2), e201–e216.

Sastry, G. M., Adzhigirey, M., & Sherman, W. (2013). Protein and ligand preparation : parameters , protocols , and influence on virtual screening enrichments. *J Comput Aided Mol Des*, *27*(3), 221–234.

Sawan, H. M., Al-mamoori, F., Al-samydai, A., & Mayyas, A. (2024). Assessment of combinations ' antimicrobial activity against Staphylococcus aureus. *Front Microbiol*, *8*(14), 1349550.

Schrödinger, L. (2023). *Schrödinger Release 2023-1: LigPrep; Schrödinger, LLC: New York, NY, USA,*.

Serdaroğlu, G. (2023). Computational Insights in Drug-likeness and ADMT Properties of -dienes Resemble of Geranial Geranial benzeri - dienlerin İlaç Benzerliği ve ADMT Özelliklerine İlişkin Hesaplamalı Analizler. *Ordu University Journal of Science and Technology*, *13*(2), 174–192.

Serhan, G., Stack, C. M., Perrone, G. G., & Morton, C. O. (2014). The polyene antifungals , amphotericin B and nystatin , cause cell death in Saccharomyces cerevisiae by a distinct mechanism to amphibian-derived antimicrobial peptides. *Ann Clin Microbiol Antimicrob*, *13*(1), 1–4.

Silverman, J. A., Perlmutter, N. G., & Shapiro, H. M. (2003). Correlation of Daptomycin Bactericidal Activity and Membrane Depolarization in Staphylococcus aureus. *Antimicrob Agents Chemother*, *47*(8), 2538–2544.

Sisto, F., Carradori, S., Guglielmi, P., Traversi, C. B., Spano, M., Sobolev, A. P., Secci, D., Carmela, M., Marcantonio, D., Haloci, E., Grande, R., & Mincione, G. (2020). Synthesis and Biological Evaluation of Carvacrol-Based Derivatives as Dual Inhibitors of H . pylori Strains and AGS Cell Proliferation. *Pharmaceuticals (Basel)*, *13*(11), 405.

Suntres, Z. E., & Coccimiglio, J. (2015). The bioactivity and toxicological actions of carvacrol. *Crit Rev Food Sci Nutr*, *55*(3), 304–318.

Tenth, A. S. (2015). *M07-A10 Methods for Dilution Antimicrobial Susceptibility Tests for Bacteria That Grow* page:88.

Theuretzbacher, U. (2011). Resistance drives antibacterial drug development. *Current Opinion in Pharmacology*, *11*(5), 433–438.

Ultee, A., Bennik, M. H. J., & Moezelaar, R. (2002). The Phenolic Hydroxyl Group of Carvacrol Is Essential for Action against the Food-Borne Pathogen Bacillus cereus. *Appl Environ Microbiol*, *68*(4), 1561–1568.

V, L. B., Heithoff, D. M., Mahan, S. P., House, J. K., & Mahan, M. J. (2023). Protocol Antimicrobial susceptibility testing to evaluate minimum inhibitory concentration values of clinically relevant antibiotics Antimicrobial susceptibility testing to evaluate minimum inhibitory concentration values of clinically. *STAR Protocols*, *4*(3), 102512.

Verhoef, J., van Kessel, K., & Snippe, H. (2019). Immune Response in Human Pathology: Infections Caused by Bacteria, Viruses, Fungi, and Parasites. In *Nijkamp and Parnham's Principles Immunopharmacology* (pp. 165–178).

Vincenzi, M. De, Stammati, A., Vincenzi, A. De, & Silano, M. (2004). Constituents of aromatic plants : carvacrol. *Fitoterapia*, *75*(7–8), 801–804.

Vitiello, A., Ferrara, F., Boccellino, M., Ponzo, A., Cimmino, C., Comberiati, E., Zovi, A., Clemente, S., & Sabbatucci, M. (2023). Antifungal Drug Resistance : An Emergent Health Threat. *Biomedicines*, *11*(4), 1063.

Wah, K., Tang, K., Millar, B. C., Moore, J. E., & Moore, J. E. (2023). Antimicrobial Resistance (AMR). *Br J Biomed Sci*, *80:11387*.

Wanda, M. (2023). Carvacrol — A Natural Phenolic Compound with Antimicrobial Properties. *Antibiotics, 12:824*.

WHO. (2007). *infectious-diseases-are-spreading-more-rapidly-than-ever-before,-who-warns*. https://www.bcm.edu/departments/molecular-virology-and-microbiology/emerging-infections-and-biodefense/introduction-to-infectious-diseases

WHO. (2011). combat antimicrobial resistance: No action today, no cure tomorrow. Remarks at a high-level panel on World Health Day 2011. *WHO Publications*. http://www.ijmr.org.in/article.asp?issn=09715916;year=2014;volume=139;issue=1;spage=1

82;epage=183;aulast=Kapi.

WHO. (2023). Antimicrobial resistance. *WHO*. https://www.who.int/news-room/fact-sheets/detail/antimicrobial-resistance.

Yao, J., & Rock, C. O. (2018). HHS Public Access. *Molecular and Cell Biology of Lipids*, *1862*(11), 1300–1309.

Zaman, A., Shampa, S. A., Ahmed, N. U., Uddin, J., Miah, A. A., Shandhi, S. P., Akter, B., & Alam, S. (2024). Carvacrol : A Prospective Gold Mine of New Drug Discovery and Development Carvacrol : A Prospective Gold Mine of New Drug Discovery and Development. *Bangladesh Pharm J*, *27*(1), 116–125.

Zhang, Y., White, S. W., & Rock, C. O. (2006). Inhibiting Bacterial Fatty Acid Synthesis*. *Journal of Biological Chemistry*, *281*(26), 17541–17544.

Appendices

Appendix1. The ^{1}H and ^{13}C NMR spectra of the synthesized compounds

^{1}H and ^{13}C NMR spectra of compound **14**

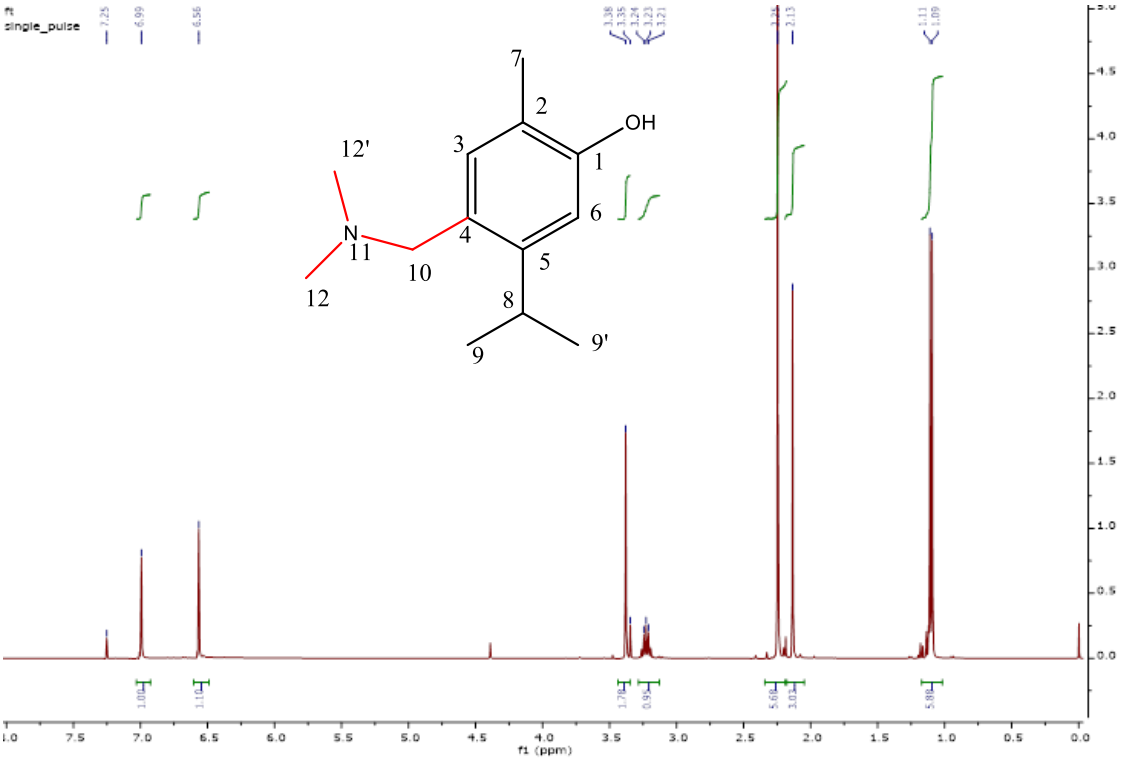

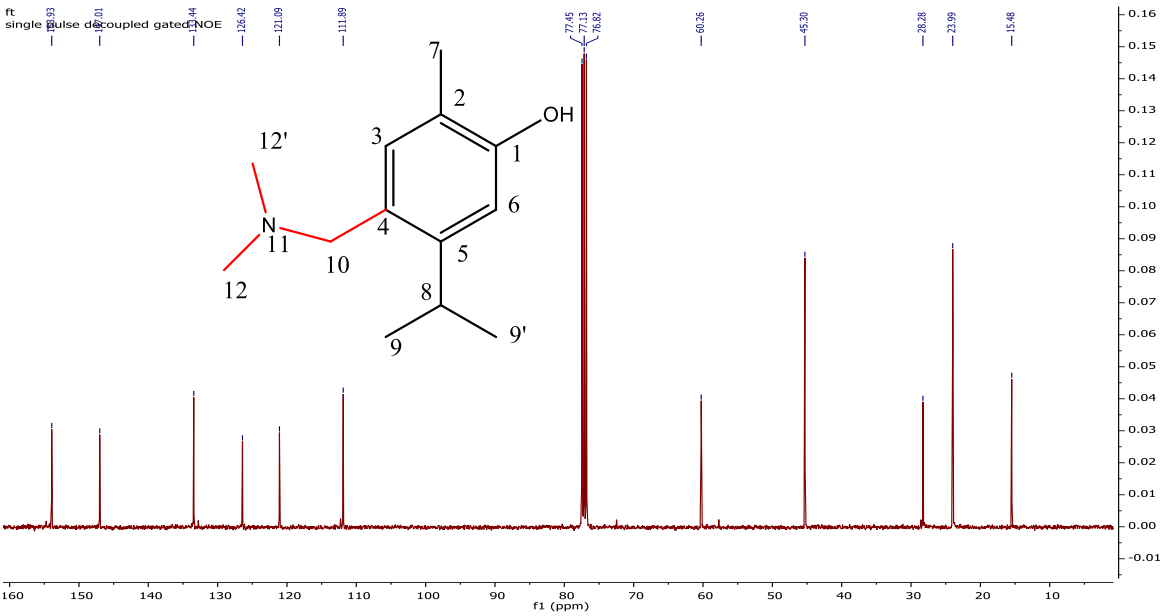

^{1}H and ^{13}C NMR spectra of compound **15**

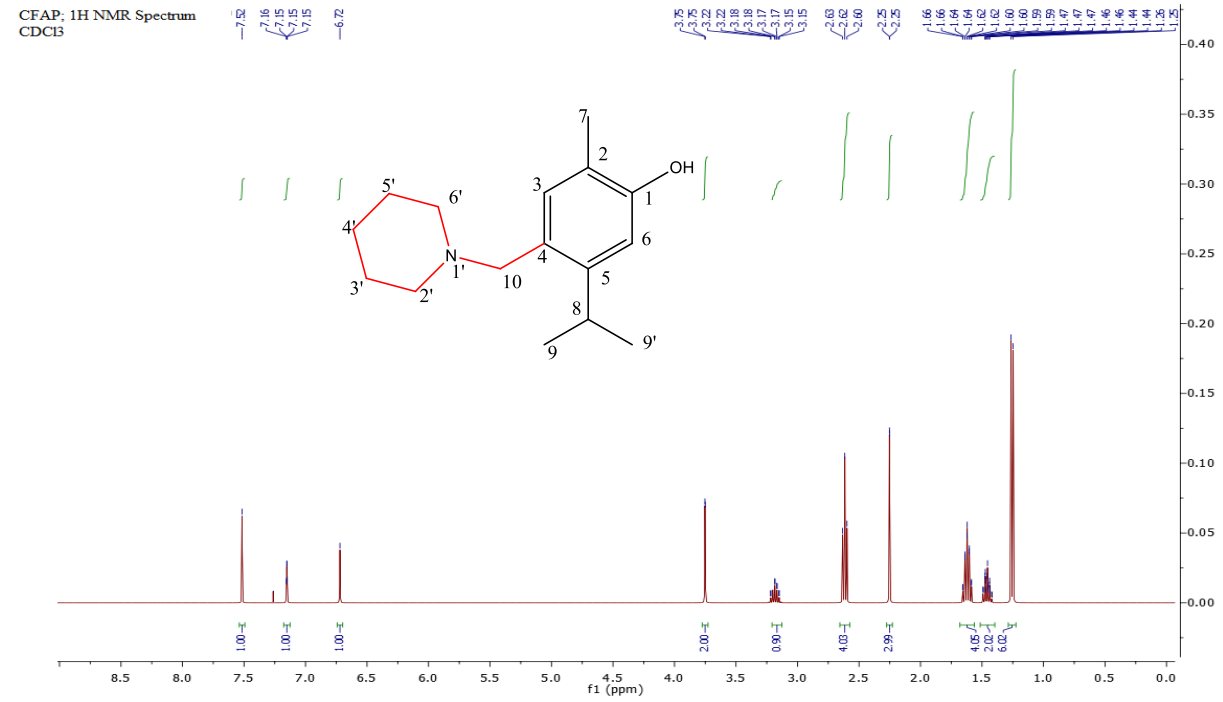

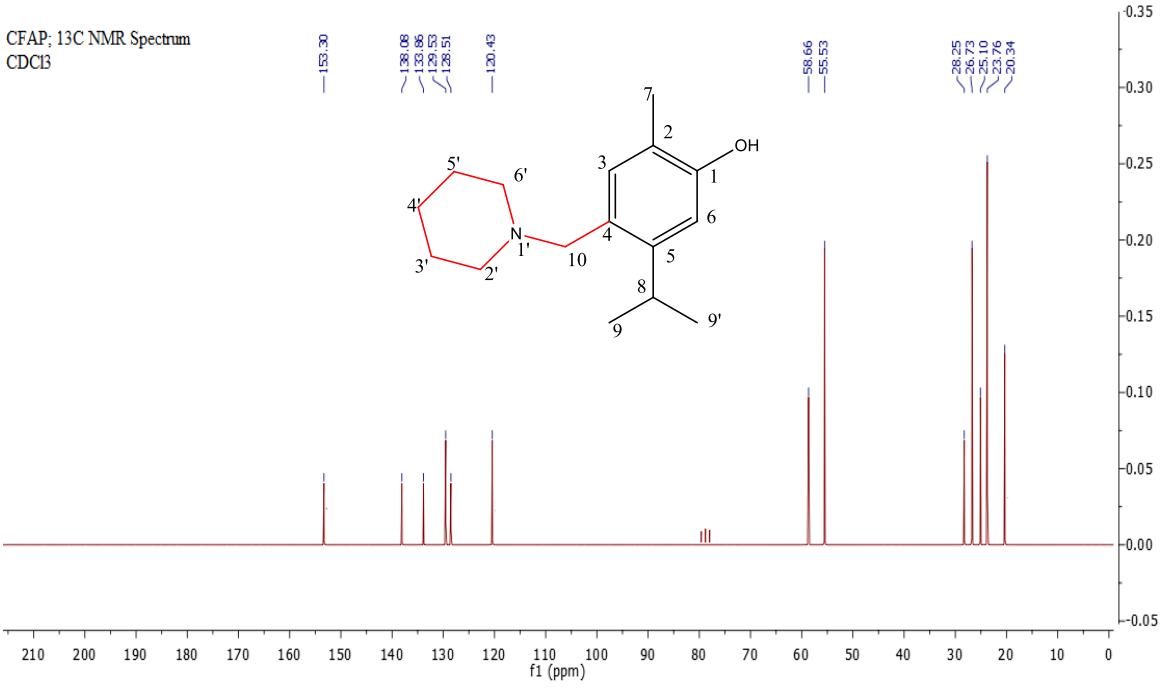

Appendix2. TLC chromatogram of synthesized compounds

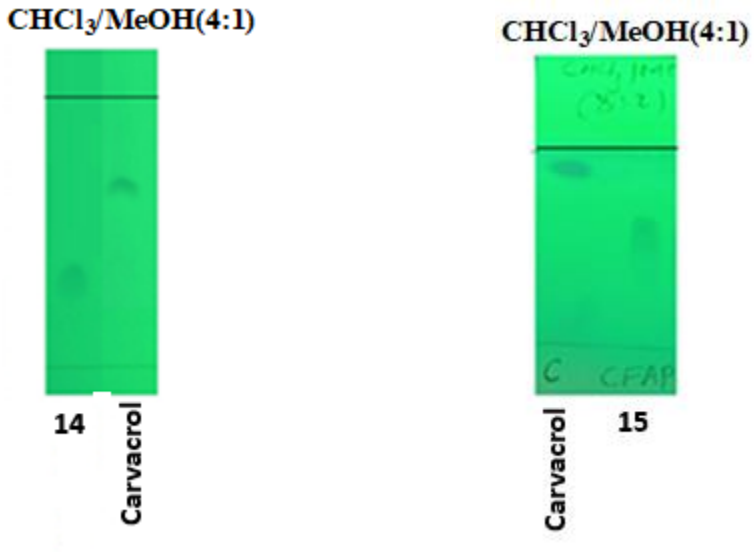

Figure: I Normal-phase TLC chromatograms of compounds 14 and 15, visualized under UV light at 254 nm.

Appendix3. Binding interactions of the compound **14**, **15** and triclosan, inhibitor of the *Escherichia coli* FabI enzyme

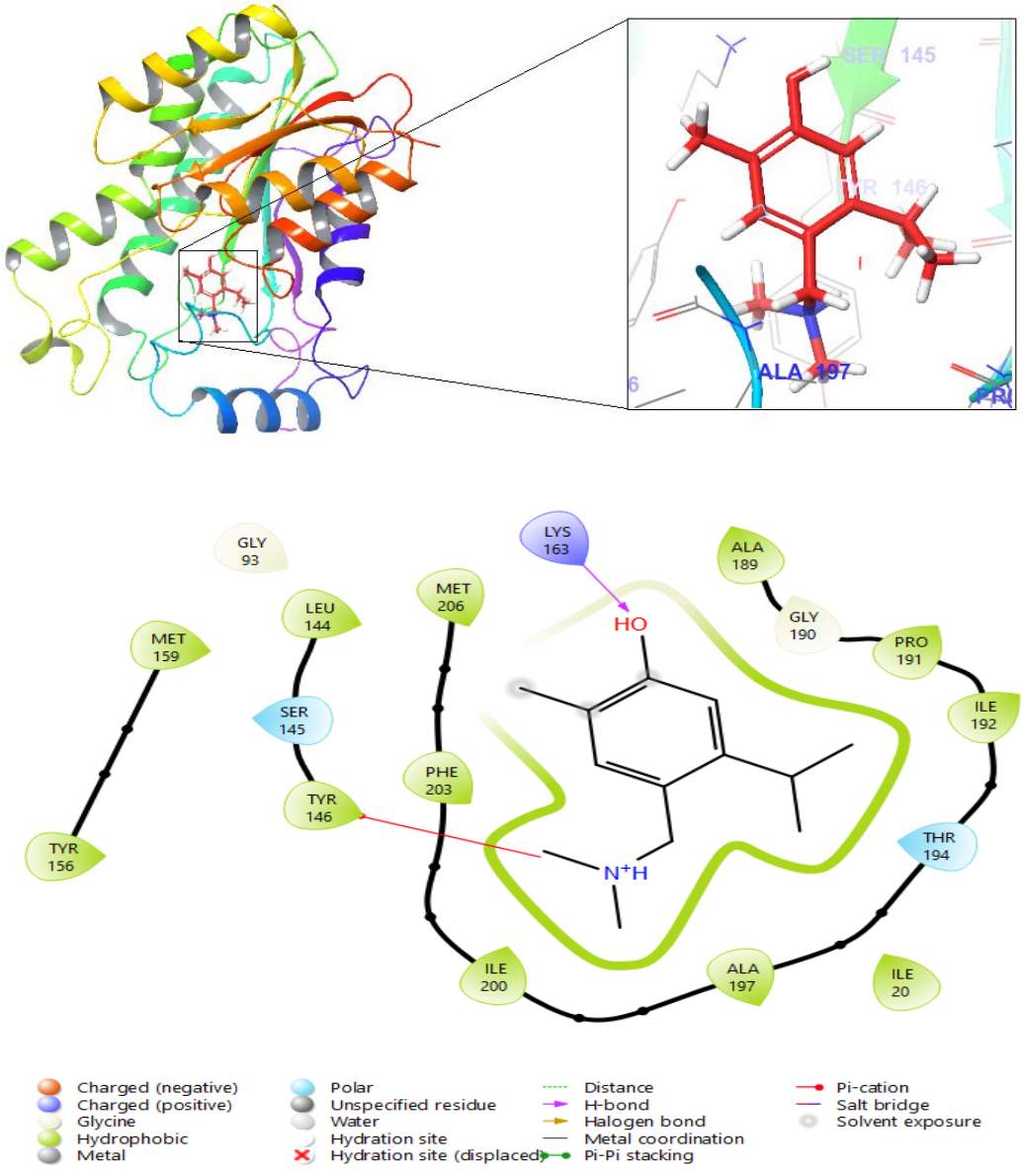

Figure I: 3D and 2D binding interaction of compound **14** with *E. coli* FabI (1C14.pdb)

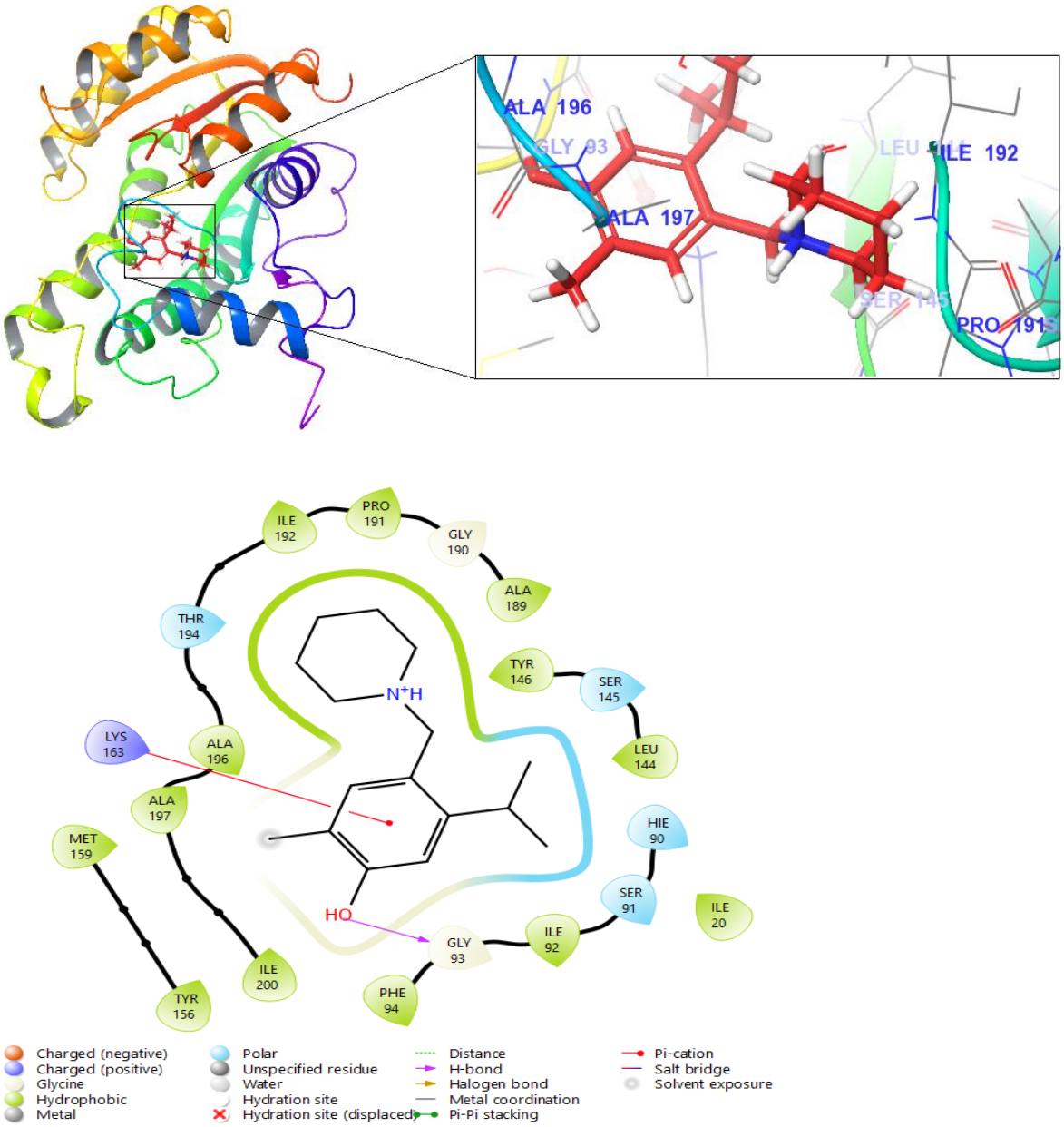

Figure II: 3D and 2D binding interaction of compound **15** with *E. coli* FabI (1C14.pdb)

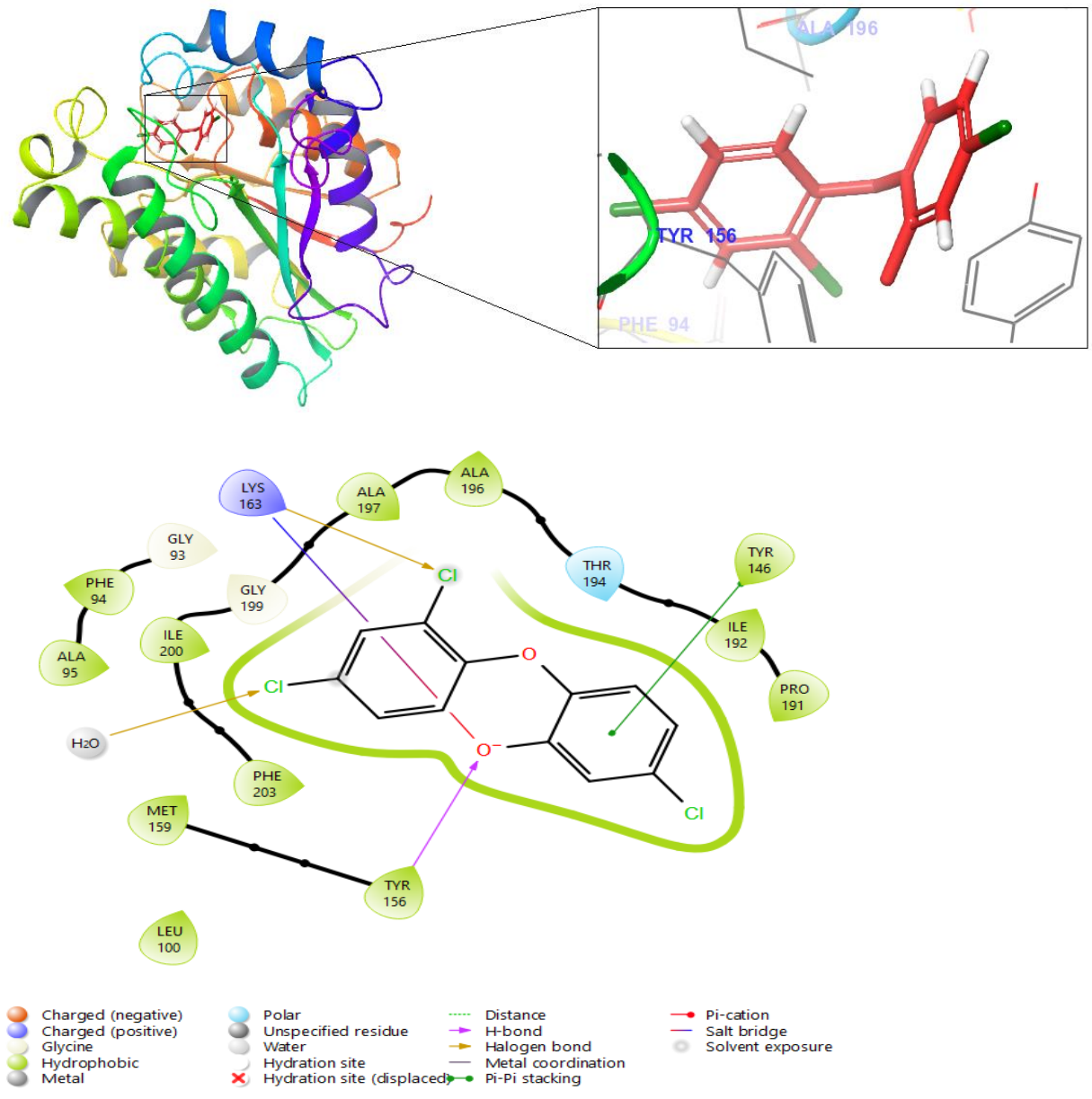

Figure I: 3D and 2D binding interaction of triclosan with *E. coli* FabI (1C14.pdb)

Manuscript

Synthesis, *In vitro* Antimicrobial and *In silico* Studies of Aminoalkyl Derivatives of Carvacrol

Asaminew Goa[1], Daniel Bisrati[1], Avijit Mazumder[2], and Kaleab Asres[1]

[1]Department of Pharmaceutical Chemistry and Pharmacognosy, School of pharmacy, College of Health Sciences, Addis Ababa University, Addis Ababa, Ethiopia;

[2]Department of Pharmaceutical Technology, Noida Institute of Engineering and Technology, 19 Knowledge Park II, Institutional Area, Greater Noida, 201306, India

Abstract

The global rise in antimicrobial resistance has created the urgent need for novel antimicrobial agents. Carvacrol, a naturally occurring phenolic compound, has garnered attention for its broad-spectrum biological activities. In this study, two new aminoalkyl derivatives of carvacrol were synthesized via a Mannich-type reaction involving formaldehyde and a secondary amine (dimethylamine or piperidine). Structural characterization using ^{1}H and ^{13}C- NMR confirmed the identities of the products as 4-((Dimethylamino)methyl)-5-isopropyl-2-methylphenol (**14**) and 5-Isopropyl-2-methyl-4-(piperidin-1-ylmethyl)phenol (**15**). Both compounds exhibited broad-spectrum antimicrobial activity against 26 bacterial and 4 fungal strains, as determined by disc diffusion and broth dilution methods. Notably, compound 15 showed the strongest antibacterial activity against *Escherichia coli* and *Vibrio cholerae* (MIC: 25 µg/mL), and potent antifungal effects against *Candida albicans* and *Penicillium funiculosum* NCTC 287 (MIC: 200 µg/mL). *In silico* studies revealed favorable drug-likeness and pharmacokinetic profiles, with compound **14** exhibiting the highest binding affinity to the bacterial FabI enzyme (docking score: –

5.677 kJ/mol). These findings highlight the potential of carvacrol-based aminoalkyl derivatives as promising candidates for antimicrobial drug development.

Keywords: Carvacrol, Aminoalkyl, Antimicrobial, Antimicrobial Resistance (AMR), Antibacterial, Antifungal, *In Silico* study

Introductions

Infectious diseases continue to pose a global health threat, particularly in low-income regions and among vulnerable populations (WHO, 2007). Bacterial infections caused 7.7 million deaths in 2019, with *S. aureus* and *E. coli* among the leading pathogens (Ikuta, 2022). Fungal diseases also present significant health risks. They can result in life-threatening systemic infections, vision loss, and chronic morbidity. Each year, fungal infections kill over 1.5 million people and affect more than a billion individuals globally (Denning, 2024). The rise of antimicrobial resistance (AMR) has further limited treatment options, with resistant infections causing over 1.27 million deaths globally in 2019 (Sartorius et al., 2024). Ethiopia faces high resistance rates among major bacterial pathogens (Berhe et al., 2021).

Natural products remain valuable in antimicrobial drug discovery. Carvacrol, a monoterpenoid phenol from oregano, exhibits notable antimicrobial activity but is limited by poor solubility, volatility, and bioavailability (Hao et al., 2021; Baranauskaite et al., 2018). Chemical modification through Mannich-type aminoalkylation can improve its pharmacological profile. In this study, aminoalkyl derivatives of carvacrol were synthesized using dimethylamine and piperidine, and evaluated for antimicrobial activity and potential mechanisms of action through in silico analysis.

Materials and Methods

Materials

Analytical-grade chemicals were obtained from Sigma-Aldrich (USA), including carvacrol, methanol, ethanol, formaldehyde (37%), chloroform, anhydrous sodium sulfate, dimethylamine, piperidine, and glacial acetic acid.

Instruments

TLC was performed on silica gel 60 F254 plates and visualized using a UV-Vis spectrophotometer (Evolution 60S). NMR spectra were acquired on a Bruker Avance DMX400 (400 MHz for ^{1}H, 100 MHz for ^{13}C) using $CDCl_3$ and TMS. Other equipment included a biosafety cabinet, incubator, refrigerator, autoclave, magnetic stirrer, analytical balance, micropipettes, and sterile microtiter plates.

Media and Standards

Media used included nutrient agar, Mueller–Hinton broth, Sabouraud dextrose agar, and broth. Ciprofloxacin and griseofulvin were used as standard antibacterial and antifungal agents, respectively; 1% DMSO served as the negative control.

Microbial Strains

The antibacterial activity of the synthesized compounds was evaluated against a diverse panel of Gram-positive and Gram-negative bacterial strains: Gram-positive strains**:** *Bacillus pumilus* 82, *Bacillus subtilis* ATCC 6633, *Staphylococcus aureus* MDR10, *S. aureus* MDR1*, *S. aureus* MDR2*. Gram-negative strains**:** *Escherichia coli* NCTC 5933, K88, NCTC 7360, LT37, 872, ROW 7/12, 3:37C, CD/99/1, HB101*, C600*, *Salmonella typhi* Ty2, *Salmonella enterica* TD01,

Shigella dysenteriae 8, *Shigella sonnei* 1, *Shigella boydii* D13629, *Shigella flexneri* Type 6, *Vibrio cholerae* NCTC 4693, NCTC 5596, NCTC 10732, NCTC 11501, *Pseudomonas aeruginosa* MDR1* All strains were obtained from the Department of Technology, Jadavpur University; Central Drugs Laboratory, Kolkata; and the Institute of Microbial Technology (IMTECH), Chandigarh, India. The strains were authenticated using standard cultural, morphological, and biochemical tests prior to screening.

Antifungal activity was assessed against the following strains: *Candida albicans* ATCC 10231, *Aspergillus niger* ATCC 6275, *Penicillium notatum* ATCC 11625, and *Penicillium funiculosum* NCTC 287. All fungal strains were procured from the Central Drugs Laboratory, Kolkata, and IMTECH, Chandigarh.

Methods

Synthesis of Aminoalkyl Derivatives of Carvacrol (14 and 15)

Synthesis of 4-((Dimethylamino)methyl)-5-isopropyl-2-methylphenol (Compound 14)

A solution of 37% aqueous formaldehyde (0.75 mL, 0.01 mol) in 10 mL methanol was prepared in a 50 mL beaker, with five drops of glacial acetic acid added as catalyst. Dimethylamine (0.66 mL, 0.01 mol) was added dropwise to the formaldehyde solution to generate the iminium intermediate, which was then slowly added to a solution of carvacrol (1.5 g, 0.01 mol) in methanol. The mixture was stirred and refluxed at 100 °C for 28 hours in a 250 mL Erlenmeyer flask. Progress of the reaction was monitored using TLC with chloroform: methanol (4:1) as the solvent system. Upon completion, the reaction mixture was cooled, poured into ice-cold water, and kept overnight to allow precipitation. The resulting solid was filtered, washed with ethanol,

dried over anhydrous sodium sulfate, and purified by recrystallization in ethanol to obtain pure compound 14.

Synthesis of 5-Isopropyl-2-methyl-4-(piperidin-1-ylmethyl)phenol (Compound (15)

Compound **15** was synthesized following a procedure similar to that used for compound **14**. A solution of 37% aqueous formaldehyde (0.75 mL, 0.01 mol) in 10 mL of methanol was prepared with five drops of acetic acid as a catalyst. Piperidine (1 mL, 0.01 mol) was added dropwise to form the iminium intermediate, which was then added dropwise to a methanolic solution of carvacrol (1.5 g, 0.01 mol). The reaction mixture was stirred and refluxed at 100°C for 20 hours, with reaction progress monitored by TLC. After refluxing, the mixture was cooled and poured into ice-cold water, then stored overnight in the refrigerator. The resulting precipitate was filtered, washed with ethanol, dried over anhydrous Na_2SO_4, and recrystallized from ethanol to obtain pure compound **15.**

In Vitro Antimicrobial Assays

Disc Diffusion Assay

The antibacterial and antifungal activities were initially evaluated using the disc diffusion method (Mitchell, J.K. and Carter, 2000). Stock solutions of the test compounds were prepared at 200 µg/mL in 1% DMSO. Sterile Petri dishes containing solidified nutrient agar (for bacteria) or SDA (for fungi) were inoculated with standardized microbial suspensions (adjusted to 0.5 McFarland standards). Sterile 6 mm filter paper discs (Whatman No. 1) were soaked in the test solutions and placed onto the inoculated agar surfaces. Plates were incubated at 37 °C for 24 hours for bacterial cultures and at room temperature for three days for fungal cultures. Zones of inhibition (ZOI) were measured in millimeters. Ciprofloxacin and griseofulvin served as positive

controls for antibacterial and antifungal assays, respectively, while 1% DMSO was used as the negative control (H & D, 2010).

Broth Dilution Method

Minimum inhibitory concentrations (MICs) were determined by broth dilution according to established protocols Jean B.etal (2015). Serial dilutions of the test compounds were prepared in MHB (for bacteria, 5–800 µg/mL) and SDB (for fungi, 50–2000 µg/mL). Wells were inoculated with microbial suspensions and incubated at 37 °C for 24 hours (bacteria) or 25 °C for three days (fungi). A growth control (broth with inoculum, no test compound) and sterility control (broth only) were included. MIC was defined as the lowest concentration showing no visible turbidity (V et al., 2023).

***In silico* studies**

Molecular docking was performed using the Schrödinger Suite 2023-1 targeting enoyl-acyl carrier protein reductase (FabI, PDB ID: 1C14), a key enzyme in bacterial fatty acid biosynthesis. The protein was prepared by removing water molecules, adding hydrogens, and minimizing the structure using the OPLS4 force field (Sastry et al., 2013).. Ligands (compounds **14** and **15**) were sketched in ChemDraw, converted to 3D, and optimized in LigPrep with Epik to account for ionization and tautomeric states at pH 7.0 ± 2.0 (Schrödinger, 2023). The receptor grid was centered on the native ligand's binding site, which was removed prior to docking. Glide XP mode was used for docking with standard parameters, and redocking of the native ligand validated the protocol. Key interactions, including hydrogen bonds and hydrophobic contacts, were analyzed. Drug-likeness and ADMET profiles were predicted using ADMETlab 3.0 based on SMILES inputs, covering pharmacokinetic properties, toxicity, and compliance with Lipinski’s Rule of Five.

Results and Discussion

Synthesis of compounds 14 and 15

In this study, aminoalkyl derivatives of carvacrol were successfully synthesized by carrying out a Mannich-type reaction. In this process, carvacrol was reacted with formaldehyde and two different secondary amines—dimethylamine and piperidine. This reaction involved the formation of an aminoalkyl group attached to the aromatic ring of carvacrol, resulting in the corresponding aminoalkylated products (**14** and **15**).

Table 8: Physical properties of the compounds **14** and **15**

Compound	Molecular Formula	Predicted MW(g/mol)	Physical State	Color	% Yield	Rf value
14	$C_{13}H_{21}NO$	207.31	Crystal	Colorless	85	0.45
15	$C_{16}H_{25}NO$	247.19	Crystal	Colorless	67	0.55

Structural confirmation of synthesized compounds 14 and 15

The structures of compounds **14** and **15** were determined using ^{1}H-NMR and ^{13}C-NMR spectral data.

4-((Dimethylamino)methyl)-5-isopropyl-2-methylphenol (14)

The ^{1}H-NMR spectrum of compound **14** displayed two aromatic proton signals, assigned to H-6 (δ 6.56, ArH, *s*) and H-3 (δ 6.99, ArH, *s*), indicating that one of the aromatic protons in carvacrol was replaced by an aminoalkyl group. This confirms that the reaction occurred on the aromatic ring through substitution of one proton. Furthermore, a signal at δ 3.38 (2H, *s*) indicated the presence of a methylene group attached to a nitrogen atom, suggesting the formation of an aminoalkyl group in compound **14**.

The ^{13}C-NMR confirmed the presence of a total of 13 carbon atoms in compound **14**. These included four quaternary carbons, five methyls (5xCH_3), three methines (3xCH), and one methylene (CH_2). The methylene carbon linking the aromatic ring to the dimethylamino group appeared at δC 60.26 ppm. The ^{1}H NMR spectrum, combined with the ^{13}C- NMR data, confirms the proposed structure of 4-((dimethylamino) methyl)-5-isopropyl-2-methylphenol. The chemical shifts of all other protons and carbons in compound **14** are detailed in the Table 2.

5-Isopropyl-2-methyl-4-(piperidin-1-ylmethyl) phenol (15)

The ^{1}H-NMR spectra of compound **15** showed two aromatic protons, identified as H-6 (δ 6.72, 1H, *s*) and H-3 (δ 7.15, 1H, *s*). Additionally, one aromatic proton in carvacrol, which originally contained three aromatic protons, was replaced by an alkyl group. A singlet at δ of 3.75 ppm corresponded to the methylene (-CH_2-) group at position 10, linking the aromatic ring to the piperidine moiety, while signals at δ of 2.62, 1.47, and 1.66 ppm corresponded to protons at positions 2'and 6', 3' and 5', and 4', respectively, within the piperidine ring.

The ^{13}C-NMR confirmed the presence of a total of 16 carbon atoms in compound **15**. These included four quaternary carbons, three methyl carbons (3xCH_3), three methane carbons (3xCH), and six methylene carbons (CH_2). The methylene carbon linking the aromatic ring to the piperidine group was found at δ C 58.66 ppm, and the methylene carbons of the piperidine ring were observed at δ C 25.1, 26.73, and 55.53 ppm. Based on the combined ^{1}H and ^{13}C-NMR spectral data, compound **15** was identified as 5-isopropyl-2-methyl-4-(piperidin-1-ylmethyl) phenol. The remaining chemical shifts for both protons and carbons are provided in the Table 2.

Table 9: 1H and 13C-NMR spectral data of synthesized compounds

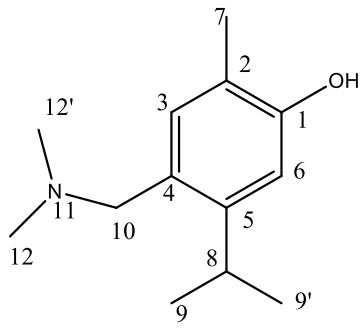

Compound **14**

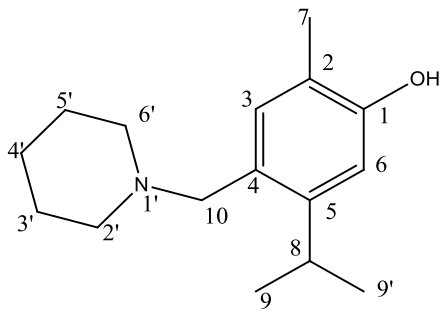

Compound **15**

Position	δ H (ppm)	δ C (ppm)	Position	δ H (ppm)	δ C (ppm)
1		153.93	1		153.30
2		121.09	2		128.51
3	6.99 (ArH, s)	133.44	3	7.15 (ArH, *s*)	133.86
4		126.42	4		129.53
5		147.01	5		138.08
6	6.56(ArH, s)	111.89	6	6.72 (ArH, *s*)	120.43
7	2.13(3H, *s*)	15.48	7	2.25(3H,*s*)	20.34
8	3.21(1H,*m*)	28.26	8	3.17 (1H, *m*):	28.25
9,9'	1.1(3H,3H,*d*, J = 8 Hz)	23.99	9,9'	1.26 (3H.3H, *d*, J = 8 Hz)	23.76
10	3.38(2H,*s*)	60.25	10	3.75(2H,s)	58.66
12,12'	2.25(3H,3H,*s*)	45.30	2', 6'	2.62(4H,*t*)	55.53
			3', 5'	1.66(4H,*m*)	26.73
			4'	1.47 (2H,*m*)	25.1

Antimicrobial activity of compound 14 and 15

Antibacterial activity

Compounds **14** and **15** were tested against 26 bacterial strains using disc diffusion (200 µg/mL) and broth dilution methods. Ciprofloxacin served as the reference drug. Both compounds exhibited broad-spectrum antibacterial activity, with inhibition zones of 6–16 mm and MICs ranging from 25 to 400 µg/mL (Table 3). Compound **15** showed consistently stronger activity than compound **14**, particularly against *E. coli* (ZOI: 12.5–16 mm; MIC: 25–100 µg/mL) and *Vibrio cholerae* (ZOI: 15.5–16 mm; MIC: 25 µg/mL). Moderate activity was observed against *Salmonella* and *Shigella spp.* (MIC: 100–200 µg/mL). Both compounds were inactive against

Bacillus pumilus and B. subtilis. While some activity was noted against *S. aureus* MDR10 (MIC: 50 µg/mL), resistance was higher in MDR1 and MDR2 strains (MIC: 400 µg/mL). Overall, compound **15** demonstrated enhanced efficacy, especially against Gram-negative pathogens

Table 10: Zone of inhibition and minimum inhibitory concentration of the compound 14 and 15 against the tested bacterial strains

Name of Bacteria	Zone of inhibition in mm (200 µg/ml)			MIC (µg/ml)	
	Compound **14**	Compound **15**	Ciprofloxacin	Compound **14**	Compound **15**
E.coli NCTC 5933	13.0	15.0	16.0	50	25
E.coli K88	13.5	14.5	17.0	50	25
E.coli NCTC 7360	14.0	15.0	17.0	50	25
E.coli LT37	13.5	15.5	16.0	50	25
E.coli 872	14.0	15.0	16.0	50	25
E.coli ROW 7/12	14.0	15.5	16.5	50	25
E.coli 3:37C	14.5	16.0	16.5	50	25
E.coli CD/99/1	14.0	15.5	17.0	50	25
*E.coli HB101**	12.0	12.5	14.0	200	100
*E.coli C600**	11.5	13.0	13.5	200	100
Salmonella typhi Ty2	13.5	13.5	16.0	100	100
Salmonella enterica TD 01	13.5	13.5	19.0	100	100
Shigella dysentery 8	11.5	12.0	20.0	200	100
Shigella soneii 1	13.0	12.5	19.5	200	100
Shigella boydii D13629	12.0	12.0	20.0	200	100
Shigella flexneri Type 6	12.0	13.0	20.5	200	100
Staphylococcus aureus MDR10	13.5	13.0	18.0	50	50
*S.aureus MDR 1**	10.0	9.5	11.5	200	400
*S.aureus MDR 2**	11.5	10.0	12.0	200	400
Bacillus pumilus 82	6.0	6.0	19.0	NA	NA
Bacillus subtilis ATCC 6633	6.0	6.0	18.0	NA	NA
Vibrio cholerae NCTC 4693	14.0	15.5	17.5	50	25
Vibrio cholerae NCTC5596	14.5	16.0	18.5	50	25
Vibrio cholerae NCTC 10732	14.5	16.0	19.0	50	25
Vibrio cholerae NCTC 11501	14.5	15.5	18.5	50	25
*Pseudomonas aeruginosa MDR 1**	10.5	10.0	12.5	100	400

NA; no activity

Antifungal activity

Both synthesized compounds demonstrated antifungal activity against four fungal strains, with zones of inhibition ranging from 10.5 to 14.5 mm and MIC values between 200 and 800 µg/mL

as summarized in Table 4. Overall, compound **15** exhibited stronger antifungal activity than compound **14** across all tested strains. Among the fungi evaluated, *Candida albicans* ATCC 10231 (ZOI= 14.5mm and MIC= 200 µg/mL) and *Penicillium funiculosum* NCTC 287 (ZOI= 13.5mm and MIC= 200) were the most susceptible to compound **15**, showing the largest zone of inhibition (14.5 mm) and the lowest MIC (200 µg/mL), indicating notable antifungal potency. A comparative assessment of both compounds revealed differences in activity levels against the tested fungal strains (Table 4).

Table 11: Zone of inhibition and minimum inhibitory concentration of the compound 14 and 15 against the tested fungal species

Name of Fungi	Zone of inhibition in mm(2000µg/ml)			MIC(µg/ml)	
	Compound **14**	Compound **15**	Griseofulvin	Compound **14**	Compound **15**
Candida albicans ATCC 10231	12.0	14.5	16.0	400	200
Aspergillus niger ATCC 6275	11.0	14.0	15.0	800	400
Penicillium notatum ATCC 11625	11.0	13.0	13.5	800	400
Penicillium funiculosum NCTC 287	10.5	13.5	14.0	800	200

In silico analysis

Molecular docking analysis

Molecular docking of compound **14** with *E. coli* FabI (PDB ID: 1C14) revealed a favorable binding affinity, with a docking score of –5.677 kcal/mol and glide energy of –25.140 kcal/mol. The compound fit well within the active site, forming a hydrogen bond with Lys163 and polar interactions with Ser145 and Thr194. Hydrophobic interactions with residues such as Leu144, Met159, Tyr156, and Phe203, along with a π–cation interaction with Tyr146, further stabilized the binding. These interactions suggest that compound **14** may inhibit FabI by blocking the NADH binding site or substrate access.

Compound **15** exhibited favorable binding with *E. coli* FabI (PDB ID: 1C14), with a docking score of –4.976 kcal/mol and glide energy of –29.372 kcal/mol. Key interactions included a hydrogen bond with Gly93 and polar contacts with HIE90, Ser91, Ser145, and Thr194. Hydrophobic interactions and π–π stacking with Lys163 further stabilized the binding. These interactions suggest that compound **15** may interfere with NADH binding or substrate access. Redocking of triclosan (docking score: –7.194 kcal/mol) validated the docking protocol.

Table 12: Docking scores and glide energy of synthesized compounds

Ligand	**Docking score (kcal/mol)**	**Glide energy (kcal/mol)**	**Key Interactions**	
			H-bonds	None H-bonds
Compound **14**	-5.677	-25.140	Lys163	Tyr146, Ser145, Thr194
Compound **15**	-4.976	-29.372	Gly93	Lys 163, HIE90, Ser91, Ser145, Thr194
Triclosan	-7.194	-35.771	Thr194	Lys163, Tyr146

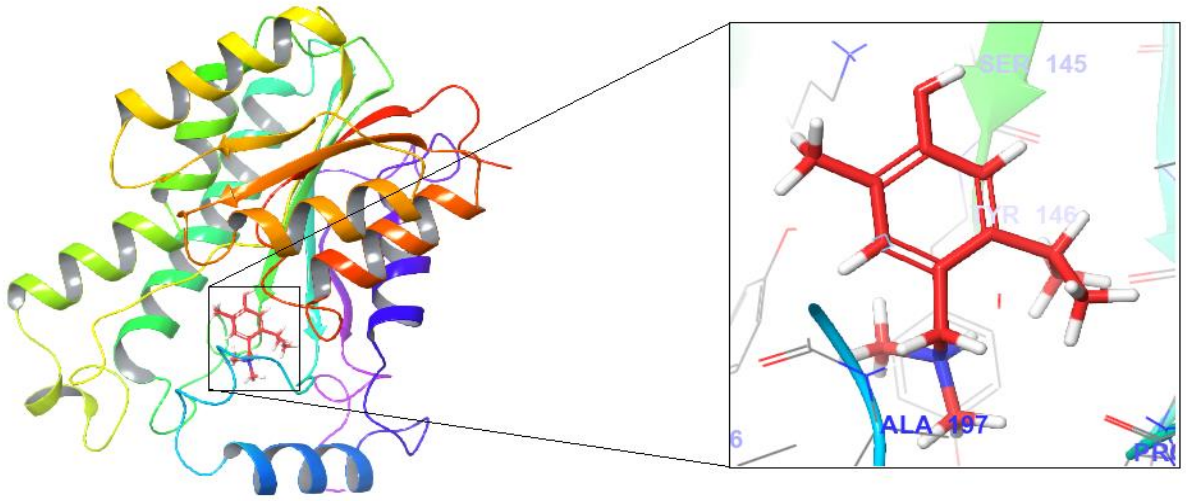

Figure 1: 3D interaction between compound **14** and *E. coli* FabI (PDB ID: 1C14)

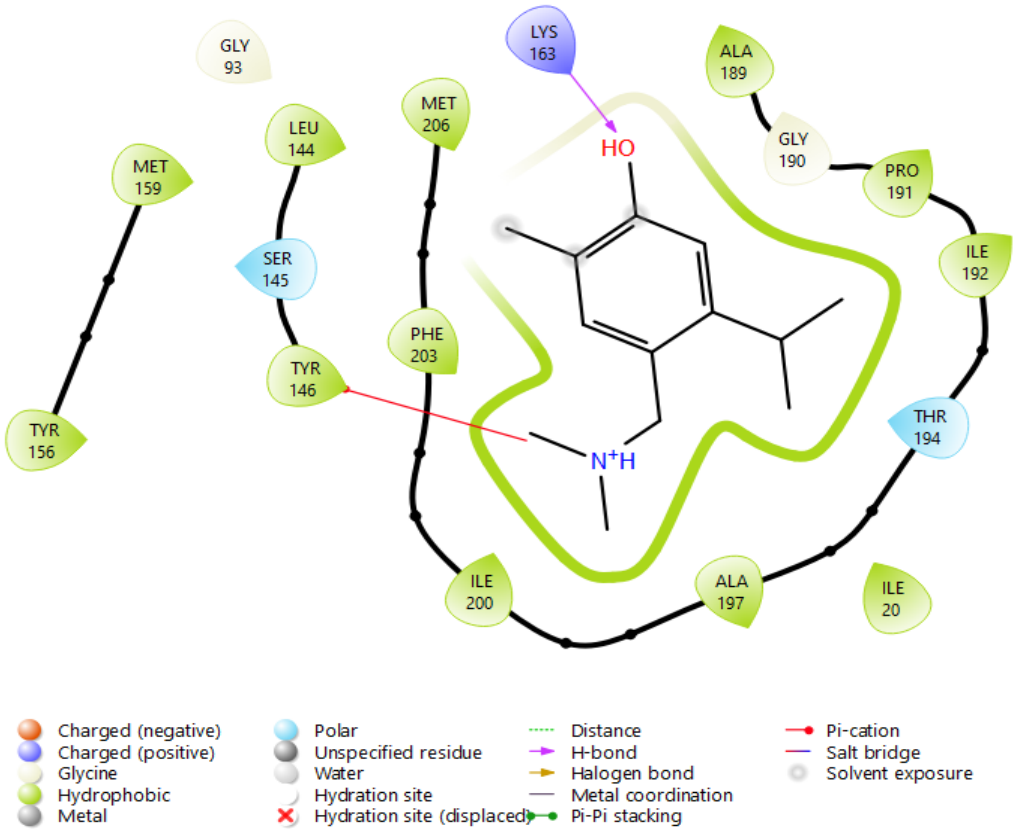

Figure 2: 2D interaction between compound **14** and E. coli FabI (PDB ID: 1C14)

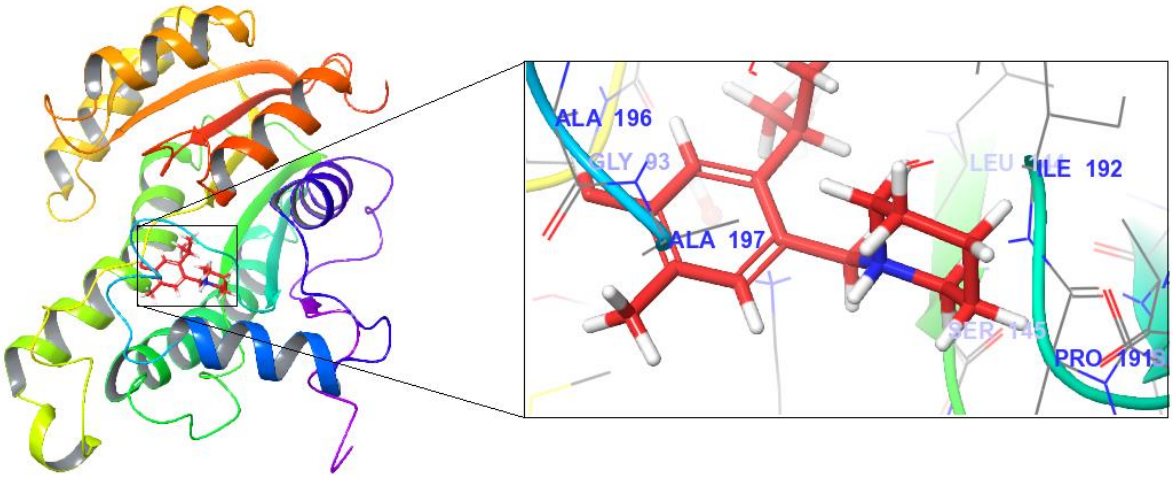

Figure 3: 3D interaction between compound **15** and *E. coli* FabI (PDB ID: 1C14)

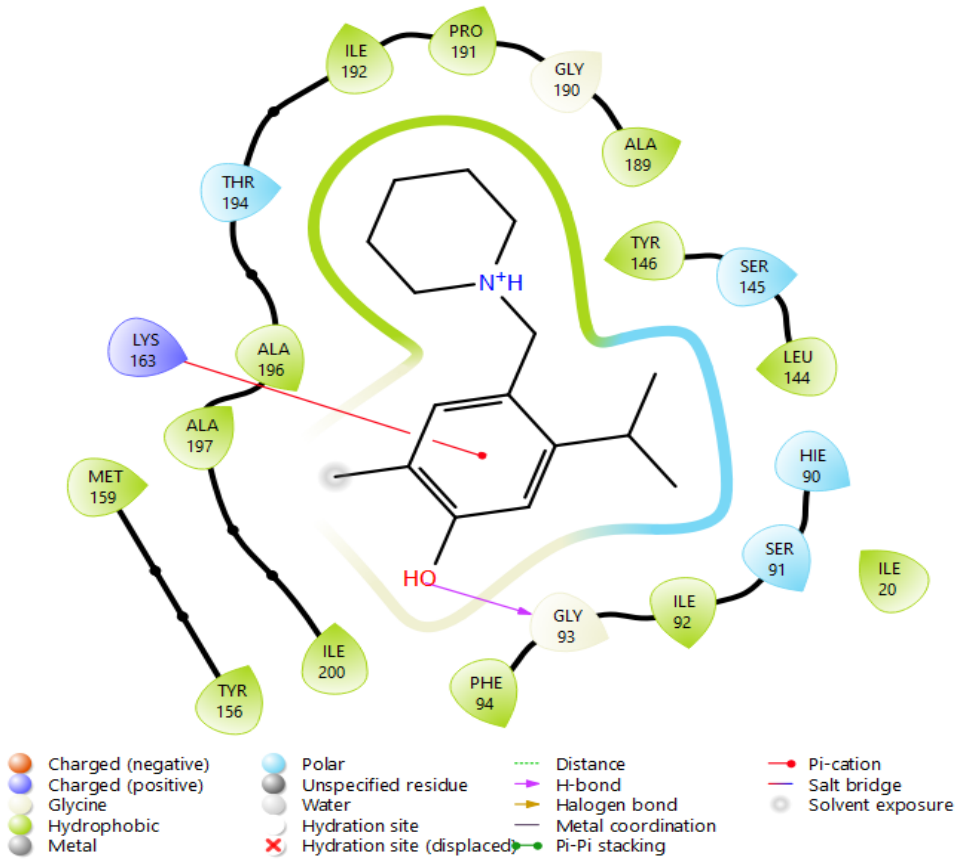

Figure 4: 2D interaction between compound **15** and *E. coli* FabI (PDB ID: 1C14)

Drug-Likeness

Physicochemical and medicinal chemistry properties are critical for assessing drug-likeness, with early prediction such as via Lipinski's Rule of Five enhancing success in lead optimization. Parameters like solubility, lipophilicity, hydrogen bonding, molecular flexibility, and synthetic accessibility inform oral bioavailability and pharmacokinetics (Lipinski et al., 2001; Serdaroğlu, 2023).. Using ADMET Lab 3.0, compounds **14** and **15** were analyzed (Table 6) and showed values within acceptable ranges. Compound **14** exhibited excellent aqueous solubility and moderate lipophilicity, while compound **15** was slightly more lipophilic but remained within limits. Both compounds met Lipinski's criteria and had favorable hydrogen bonding profiles, TPSA (23.47 $Å^2$), and flexibility—supporting good permeability. High QED scores and low synthetic accessibility values further suggest strong drug-likeness and feasibility for synthesis, making them promising drug candidates**.**

Table 13: physicochemical, and drug-likeness properties the synthesized compound

Parameters	Compound **14**	Compound **15**	Triclosan	Reference Range	Interpretation
nHA (H-bond acceptors)	2	1	2	0–12	Both are within acceptable range.
nHD (H-bond donors)	1	1	1	0–7	Indicates acceptable H-bonding for oral bioavailability.
nRot (rotatable bonds)	3	3	2	0–11	Suggests moderate molecular flexibility.
TPSA ($Å^2$) (topological polar surface area)	23.47	23.47	29.46	0–140	Low TPSA, favorable for membrane permeability and oral absorption.
LogS (solubility)	-2.535	-3.469	-4.555	-4 to 0.5	Compound 14 has better aqueous solubility; both are within range.
LogP (lipophilicity)	2.789	3.774	4.512	0–3	Compound 14 has moderate lipophilicity; compound 15 is slightly above the ideal.
LogD (distribution at pH 7.4)	2.36	3.234	3.494	1–3	Both compounds show good membrane permeability; compound 15 is near upper limit.
Lipinski's Rule of 5	Accepted	Accepted	Accepted	—	Indicates good oral drug-likeness.
QED (quantity estimate of drug-likeness)	0.823	0.878	0.829	>0.67	High QED scores indicate strong drug-like properties.
SA score (synthetic access)	2	2	1	≤6	Both are synthetically accessible.

ADMET Properties

In silico ADMET prediction plays a vital role in drug discovery by guiding the optimization of lead compounds. Using ADMET Lab 3.0, the pharmacokinetic and toxicity profiles of compounds **14** and **15** were assessed, with results summarized in Table 7 (Fu et al., 2024). Key parameters included absorption, distribution, metabolism, elimination, and toxicity, such as BBB permeability, gastrointestinal absorption, P-glycoprotein (P-gp) interaction, and CYP450 enzyme inhibition.

Both compounds demonstrated strong Caco-2 permeability (above –5.15 cm/s) and excellent human intestinal absorption (HIA < 0.01), indicating good oral bioavailability. Neither compound is a P-gp substrate, suggesting favorable intracellular retention and reduced efflux (Lin & Yamazaki, 2003). The volume of distribution (VDss) values 0.454 L/kg for compound **14** and 0.617 L/kg for compound **15** were within the acceptable range (0.04–20 L/kg).

Compound **15** exhibited higher BBB permeability (0.66), indicating better central nervous system (CNS) penetration than compound **14** (0.462). Both compounds showed no inhibitory activity against CYP1A2, CYP2C19, and CYP2C8, suggesting low potential for metabolic drug–drug interactions. Clearance predictions were favorable, though compound **14** had a slightly prolonged half-life (0.964), indicating potentially extended systemic exposure (Benet et al., 2002).

Toxicity modeling revealed low hERG inhibition and minimal p53 activation for both compounds, suggesting low cardiotoxic and genotoxic risk. Compound **15** also exhibited a lower Ames mutagenicity score than compound **14**, indicating a better safety profile.

Table 13: Prediction of ADMET properties of the synthesized compounds

Parameter	Compound **14**	Compound **15**	Triclosan	Recommended Range	Interpretation
Caco-2 permeability	-4.765	-4.725	-4.805	> -5.15	Good intestinal permeability predicted for both.
PPB (%plasma protein bound)	82.545%	86.3%	99.158%	< 90%	Acceptable plasma protein binding.
HIA (absorption)	0.0	0.0	0.0	0.0–0.1	Good human intestinal absorption predicted.
Pgp-substrate	0.055	0.018	0.004	0.0–0.1	Low risk of P-glycoprotein efflux; favorable for oral bioavailability.
VDss (L/kg)	0.454	0.617	-0.149	0.04–20	Moderate volume of distribution.
BBB permeability	0.462	0.66	0.967	0.5–0.7	Compound 15 may cross the blood-brain barrier; compound 14 is borderline.
CYP inhibition	All values < 0.1	All values < 0.1	All values < 0.1	0.0–0.1	Both compounds are unlikely to inhibit major CYP450 enzymes favorable.
Clearance (mL/min/kg)	13.946	9.668	6.416	≥ 5	Both have acceptable drug clearance rates.
Half-life (T½)	0.964	0.465	1.139	0.3–0.7 (medium)	Compound 15 shows moderate stability; compound 14 has a slightly longer half-life.
hERG inhibition (human ether-a-go-go related gene)	0.358	0.64	0.89	0.0–0.7	Within medium risk; compound 15 closer to upper bound.
Ames test	0.413	0.248	0.246	0.0–0.3	Compound 15 shows lower mutagenic potential than 14.
SR-p53 interaction (a tumor suppressor protein p53)	0.00	0.068	0.458	0.0–0.3	Low toxicity risk for both.

Conclusion

In this study, two novel aminoalkyl derivatives of carvacrol, 4-((dimethylamino)methyl)-5-isopropyl-2-methylphenol **(14)** and 5-isopropyl-2-methyl-4-(piperidin-1-ylmethyl)phenol **(15),** were synthesized using a Mannich-type reaction. Both compounds exhibited broad-spectrum antimicrobial activity, with compound **15** demonstrating superior antimicrobial activity. For instance, compound **15** showed stronger antibacterial activity against *E. coli* (MIC: 25 μg/mL) compared to compound **14** (MIC: 50 μg/mL), highlighting its superior potency and potential as a lead compound for treating infections such as urinary tract infections, gastroenteritis, and sepsis. Additionally, it displayed potent antifungal activity against *C. albicans* and *P. funiculosum* (MIC: 200 μg/mL). Molecular docking studies revealed that both derivatives interact favorably with the active site and may inhibit the *E. coli* FabI enzyme, which plays a critical role in fatty acid elongation essential for bacterial membrane synthesis. These findings support the potential of structural modifications of carvacrol to improve its antimicrobial profile.

References

Benet, L. Z., Hoener, B., & Francisco, S. (2002). C LINICAL. *Clin Pharmacol Ther*, *71*(3), 115–121.

Berhe, D. F., Beyene, G. T., Seyoum, B., Gebre, M., Haile, K., Tsegaye, M., Boltena, M. T., Tesema, E., Kibret, T. C., Biru, M., Siraj, D. S., Shirley, D., Howe, R., & Abdissa, A. (2021). Prevalence of antimicrobial resistance and its clinical implications in Ethiopia : a systematic review. *Antimicrobial Resistance & Infection Control*, *10*(1), 168.

Denning, D. W. (2024). Global incidence and mortality of severe fungal disease. *Lancet Infect Dis*, *24*(7), e428–e438.

Fu, L., Shi, S., Yi, J., Wang, N., He, Y., Wu, Z., Peng, J., Deng, Y., Wang, W., Wu, C., Lyu, A.,

Zeng, X., Zhao, W., Hou, T., & Cao, D. (2024). ADMETlab 3 . 0 : an updated comprehensive online ADMET prediction platform enhanced with broader coverage , impro v ed perf ormance , API functionality and decision support. *Nucleic Acids Research*, *52*(W1), 422–431.

H, M. S. S., & D, H. P. (2010). Antimicrobial activity and phytochemical analysis of selected Indian folk medicinal plants. *International Journal of Pharma Sciences and Research (IJPSR)*, *1*(10), 430–434.

Hao, Y., Li, J., & Shi, L. (2021). A Carvacrol-Rich Essential Oil Extracted From Oregano (Origanum vulgare "Hot & Spicy") Exerts Potent Antibacterial Effects Against Staphylococcus aureus. *Frontiers in Microbiology*, *12:741861*(r), 1–13.

Ikuta, K. S. et al. (2022). Global mortality associated with 33 bacterial pathogens in 2019 : a systematic analysis for the Global Burden of Disease Study 2019. *The Lancet*, *400*(10369), 2221–2248.

Lin, J. H., & Yamazaki, M. (2003). Role of P-Glycoprotein in Pharmacokinetics Clinical Implications. *Clin Pharmacokinet*, *42*(1), 59–98.

Lipinski, C. A., Lombardo, F., Dominy, B. W., & Feeney, P. J. (2001). Experimental and computational approaches to estimate solubility and permeability in drug discovery and development settings. *Adv Drug Deliv Rev*, *46*(1–3), 3–26.

Mitchell, J.K. and Carter, W. . (2000). Modeling Antimicrobial Activity of Clorox (R) Using an Agar-Diffusion Test: A New Twist on an Old Experiment. *Bioscene*, *26*(3), 9–13.

Sartorius, B., Gray, A. P., Weaver, N. D., Aguilar, G. R., Swetschinski, L. R., Ikuta, K. S., Mestrovic, T., Chung, E., Wool, E. E., & Han, C. (2024). The burden of bacterial antimicrobial resistance in the WHO African region in 2019: a cross-country systematic analysis. *The Lancet Global Health*, *12*(2), e201–e216.

Sastry, G. M., Adzhigirey, M., & Sherman, W. (2013). Protein and ligand preparation : parameters , protocols , and influence on virtual screening enrichments. *J Comput Aided Mol Des*, *27*(3), 221–234.

Schrödinger, L. (2023). *Schrödinger Release 2023-1: LigPrep; Schrödinger, LLC: New York, NY, USA,*.

Serdaroğlu, G. (2023). Computational Insights in Drug-likeness and ADMT Properties of -dienes Resemble of Geranial Geranial benzeri - dienlerin İlaç Benzerliği ve ADMT Özelliklerine İlişkin Hesaplamalı Analizler. *Ordu University Journal of Science and Technology*, *13*(2), 174–192.

Tenth, A. S. (2015). *M07-A10 Methods for Dilution Antimicrobial Susceptibility Tests for Bacteria That Grow* page;88.

V, L. B., Heithoff, D. M., Mahan, S. P., House, J. K., & Mahan, M. J. (2023). Protocol Antimicrobial susceptibility testing to evaluate minimum inhibitory concentration values of clinically relevant antibiotics Antimicrobial susceptibility testing to evaluate minimum inhibitory concentration values of clinically. *STAR Protocols*, *4*(3), 102512.

WHO. (2007). *infectious-diseases-are-spreading-more-rapidly-than-ever-before,-who-warns*. https://www.bcm.edu/departments/molecular-virology-and-microbiology/emerging-infections-and-biodefense/introduction-to-infectious-diseases.